REPORT DOCUMENTATION PAGE

Form Approved OMB NO. 0704-0188

1. REPORT DATE (DD-MM-YYYY)	2. REPORT TYPE	3. DATES COVERED (From - To)
24-05-2016	Final Report	14-Feb-2012 - 14-Feb-2016

4. TITLE AND SUBTITLE
Final Report: Theory-guided Innovation of Noncarbon Two-dimensional Nanomaterials

5a. CONTRACT NUMBER
W911NF-12-1-0083

5b. GRANT NUMBER

5c. PROGRAM ELEMENT NUMBER
206022

6. AUTHORS
Zhongfang Chen

5d. PROJECT NUMBER

5e. TASK NUMBER

5f. WORK UNIT NUMBER

7. PERFORMING ORGANIZATION NAMES AND ADDRESSES
University of Puerto Rico at Rio Piedras
P. O. Box 21790

San Juan, PR 00931 -1790

8. PERFORMING ORGANIZATION REPORT NUMBER

9. SPONSORING/MONITORING AGENCY NAME(S) AND ADDRESS (ES)
U.S. Army Research Office
P.O. Box 12211
Research Triangle Park, NC 27709-2211

10. SPONSOR/MONITOR'S ACRONYM(S)
ARO

11. SPONSOR/MONITOR'S REPORT NUMBER(S)
60435-MS-REP.77

12. DISTRIBUTION AVAILIBILITY STATEMENT
Approved for Public Release; Distribution Unlimited

13. SUPPLEMENTARY NOTES
The views, opinions and/or findings contained in this report are those of the author(s) and should not contrued as an official Department of the Army position, policy or decision, unless so designated by other documentation.

14. ABSTRACT
By means of comprehensive and systematic DFT computations, we computationally designed novel 2D nanomaterials with unique structures and exceptional properties, such as Be5C2 monolayers with quasi-planaer pentacoordinate carbon, FeB6 monolayers hypercoordinate transition metal, semiconducting Group 15 monolayers, bismuth iodide monolayers, PdS2 monolayers with unprecedented structure as other transition-metal disulfides, Pentagonal B2C Monolayer, and examined their potential applications of 2D materials in nanoelectronics and mechanics, and identified promising materials as lithium ion battery electrodes, anchoring materials for lithium

15. SUBJECT TERMS
Two-dimensional nanomaterials, density functional calculations, theory-guided experiments, energy applications

16. SECURITY CLASSIFICATION OF:			17. LIMITATION OF ABSTRACT	15. NUMBER OF PAGES	19a. NAME OF RESPONSIBLE PERSON
a. REPORT	b. ABSTRACT	c. THIS PAGE			Zhongfang Chen
UU	UU	UU	UU		19b. TELEPHONE NUMBER 787-764-0000

Report Title

Final Report: Theory-guided Innovation of Noncarbon Two-dimensional Nanomaterials

ABSTRACT

By means of comprehensive and systematic DFT computations, we computationally designed novel 2D nanomaterials with unique structures and exceptional properties, such as Be5C2 monolayers with quasi-planaer pentacoordinate carbon, FeB6 monolayers hypercoordinate transition metal, semiconducting Group 15 monolayers, bismuth iodide monolayers, PdS2 monolayers with unprecedented structure as other transition-metal disulfides, Pentagonal B2C Monolayer, and examined their potential applications of 2D materials in nanoelectronics and mechanics, and identified promising materials as lithium ion battery electrodes, anchoring materials for lithium-sulfur batteries, and nanocatalysts for oxygen reduction reaction in fuel cells.

By joint efforts of theoretical and experimental studies, we have developed a convenient chemical approach to etch hexagonal boron nitride monolayers to achieve holes with defined shapes and edges, also observed and carefully analyzed the Moiré Profiles from van der Waals superstructures of boron nitride nanosheets. Moreover, we also proposed a new strategy to efficiently and effectively design and screen carbonyl-containing polycyclic aromatic hydrocarbons as cathode materials, and experimentally confirmed its validity.

Enter List of papers submitted or published that acknowledge ARO support from the start of the project to the date of this printing. List the papers, including journal references, in the following categories:

(a) Papers published in peer-reviewed journals (N/A for none)

Received		Paper
05/20/2016	58.00	Zhen Zhou, Zhongfang Chen, Qing Tang. Innovation and discovery of graphene-like materials via density-functional theory computations, Wiley Interdisciplinary Reviews: Computational Molecular Science, (09 2015): 360. doi: 10.1002/wcms.1224
05/20/2016	75.00	Shengli Zhang, Meiqiu Xie, Fengyu Li, Zhong Yan, Yafei Li, Erjun Kan, Wei Liu, Zhongfang Chen, Haibo Zeng. Semiconducting Group 15 Monolayers: A Broad Range of Band Gaps and High Carrier Mobilities, Angewandte Chemie International Edition, (01 2016): 1666. doi:
05/20/2016	74.00	Qing Peng, Liang Han, Xiaodong Wen, Sheng Liu, Zhongfang Chen, Jie Lian, Suvranu Dea . Mechanical properties and stabilities of ?-boron monolayers, Physical Chemistry Chemical Physics, (09 2015): 2160. doi:
05/20/2016	73.00	Dihua Wu, Zhaojun Xie, Zhen Zhou, Panwen Shen, Zhongfang Chen. Designing high-voltage carbonyl-containing polycyclic aromatic hydrocarbon cathode materials for Li-ion batteries guided by Clar's theory, J. Mater. Chem. A, (08 2015): 0. doi: 10.1039/C5TA05437K
05/20/2016	72.00	Fengyu Li, Kaixiong Tu, Haijun Zhang, Zhongfang Chen. Flexible structural and electronic properties of a pentagonal B2C monolayer via external strain: a computational investigation, Phys. Chem. Chem. Phys., (10 2015): 24151. doi: 10.1039/C5CP03885E
05/20/2016	71.00	Yu Wang, Yafei Li, Zhongfang Chen. Not your familiar two dimensional transition metal disulfide: structural and electronic properties of the PdS, Journal of Materials Chemistry C, (10 2015): 9603. doi: 10.1039/C5TC01345C
05/20/2016	70.00	Yunlong Liao, Kaixiong Tu, Xiaogang Han, Liangbing Hu, John W. Connell, Zhongfang Chen, Yi Lin. Oxidative Etching of Hexagonal Boron Nitride Toward Nanosheets with Defined Edges and Holes, Scientific Reports, (09 2015): 14510. doi: 10.1038/srep14510
05/20/2016	69.00	Haijun Zhang, Yandong Ma, Zhongfang Chen. Quantum spin hall insulators in strain-modified arsenene, Nanoscale, (12 2015): 19152. doi: 10.1039/C5NR05006E
05/20/2016	68.00	Fengxian Ma, Mei Zhou, Yalong Jiao, Guoping Gao, Yuantong Gu, Ante Bilic, Zhongfang Chen, Aijun Du. Single Layer Bismuth Iodide: Computational Exploration of Structural, Electrical, Mechanical and Optical Properties, Scientific Reports, (12 2015): 17558. doi: 10.1038/srep17558
05/20/2016	67.00	Zhongfang Chen, Jingxiang Zhao. Carbon-Doped Boron Nitride Nanosheet: An Efficient Metal-Free Electrocatalyst for the Oxygen Reduction Reaction, The Journal of Physical Chemistry C, (11 2015): 26348. doi: 10.1021/acs.jpcc.5b09037
05/20/2016	65.00	Yunlong Liao, Zhongfang Chen, John W. Connell, Yi Lin. Putting the holes in holey white graphene, SPIE Newsroom, (01 2016): 0. doi: 10.1117/2.1201512.006248
05/20/2016	64.00	Jingxiang Zhao, Carlos R. Cabrera, Zhenhai Xia, Zhongfang Chen. Single?sided fluorine–functionalized graphene: A metal–free electrocatalyst with high efficiency for oxygen reduction reaction, Carbon, (08 2016): 56. doi: 10.1016/j.carbon.2016.03.013

05/20/2016 63.00 Kaixiong Tu, Fengyu Li, Zhongfang Chen. Enhanced lithium adsorption/diffusion and improved Li capacity on SnS2 nanoribbons: A computational investigation,
Journal of Materials Research, (11 2015): 878. doi: 10.1557/jmr.2015.312

05/20/2016 62.00 Jingxiang Zhao, Yongan Yang, Ram S. Katiyar, Zhongfang Chen. Phosphorene as a promising anchoring material for lithium–sulfur batteries: a computational study,
J. Mater. Chem. A, (04 2016): 6124. doi: 10.1039/C6TA00871B

05/20/2016 61.00 Zhongfang Chen, Yafei Li, Yu Wang, Feng Li. Semi-metallic Be5C2 monolayer global minimum with quasi-planar pentacoordinate carbons and negative Poisson's ratio,
Nature Communications, (05 2016): 11488. doi: 10.1038/ncomms11488

05/20/2016 60.00 Yafei Li, Jianhua Hou, Kaixiong Tu, Haijun Zhang, Zhongfang Chen. FeB6 Monolayers: The Graphene-like Material with Hypercoordinate Transition Metal ,
Journal of the American Chemical Society, (05 2016): 5644. doi: 10.1021/jacs.6b01769

05/24/2013 6.00 Qihang Liu, Linze Li, Yafei Li, Zhengxiang Gao, Zhongfang Chen, Jing Lu. Tuning Electronic Structure of Bilayer MoS2 by Vertical Electric Field: A First-Principles Investigation,
The Journal of Physical Chemistry C, (10 2012): 0. doi: 10.1021/jp307124d

05/24/2013 18.00 JIACHENG FENG, FENGYU LI, PENG JIN, YUNLONG LIAO, ZHONGFANG CHEN. SEARCHING FOR NEW MEMBERS OF C,
Journal of Theoretical and Computational Chemistry, (02 2013): 0. doi: 10.1142/S0219633612500976

05/24/2013 17.00 Yunlong Liao, Clara Leticia Cruz, Paul von Ragué Schleyer, Zhongfang Chen. Many M©Bn boron wheels are local, but not global minima,
Physical Chemistry Chemical Physics, (2012): 0. doi: 10.1039/c2cp41521f

05/24/2013 16.00 Zhongfang Chen, Judy I. Wu, Clémence Corminboeuf, Jonathan Bohmann, Xin Lu, Andreas Hirsch, Paul von Ragué Schleyer. Is C60 buckminsterfullerene aromatic?,
Physical Chemistry Chemical Physics, (2012): 0. doi: 10.1039/c2cp42146a

05/24/2013 15.00 Fengyu Li, Peng Jin, De-en Jiang, Lu Wang, Shengbai B. Zhang, Jijun Zhao, Zhongfang Chen. B80 and B101–103 clusters: Remarkable stability of the core-shell structures established by validated density functionals,
The Journal of Chemical Physics, (2012): 0. doi: 10.1063/1.3682776

05/24/2013 14.00 Yuan Liu, Jijun Zhao, Fengyu Li, Zhongfang Chen. Appropriate description of intermolecular interactions in the methane hydrates: An assessment of DFT methods,
Journal of Computational Chemistry, (01 2013): 0. doi: 10.1002/jcc.23112

05/24/2013 13.00 Jia Guan, Wei Chen, Yafei Li, Guangtao Yu, Zhiming Shi, Xuri Huang, Chiachung Sun, Zhongfang Chen. An Effective Approach to Achieve a Spin Gapless Semiconductor–Half-Metal–Metal Transition in Zigzag Graphene Nanoribbons: Attaching A Floating Induced Dipole Field via p – p Interactions,
Advanced Functional Materials, (03 2013): 0. doi: 10.1002/adfm.201201677

05/24/2013 12.00 Ivan A. Popov, Yafei Li, Zhongfang Chen, Alexander I. Boldyrev. "Benzation" of graphene upon addition of monovalent chemical species,
Physical Chemistry Chemical Physics, (2013): 0. doi: 10.1039/c3cp43921f

05/24/2013 11.00 Qing Tang, Zhen Zhou, Zhongfang Chen. Graphene-related nanomaterials: tuning properties by functionalization,
Nanoscale, (2013): 0. doi: 10.1039/c3nr33218g

05/24/2013 10.00 Yafei Li, Zhongfang Chen. XH/? (X = C, Si) Interactions in Graphene and Silicene: Weak in Strength, Strong in Tuning Band Structures,
The Journal of Physical Chemistry Letters, (01 2013): 0. doi: 10.1021/jz301821n

05/24/2013 8.00 Fengyu Li, Zhongfang Chen. Tuning electronic and magnetic properties of MoO3 sheets by cutting, hydrogenation, and external strain: a computational investigation,
Nanoscale, (2013): 0. doi: 10.1039/c3nr33009e

05/24/2013 7.00 Qing Tang, Zhen Zhou, Panwen Shen, Zhongfang Chen. Band Gap Engineering of BN Sheets by Interlayer Dihydrogen Bonding and Electric Field Control,
ChemPhysChem, (04 2013): 0. doi: 10.1002/cphc.201300141

08/12/2013 19.00 Yafei Li, Zhen Zhou, Carlos R. Cabrera, Zhongfang Chen. Preserving the Edge Magnetism of Zigzag Graphene Nanoribbons by Ethylene Termination: Insight by Clar's Rule,
Scientific Reports, (6 2013): 0. doi: 10.1038/srep02030

08/13/2012 1.00 YUNLONG LIAO, ZHONGFANG CHEN. UNIFORM BENDING EFFECT ON ELECTRONIC PROPERTIES OF BORON NITRIDE NANORIBBONS: A COMPUTATIONAL INVESTIGATION,
Nano LIFE, (06 2012): 0. doi: 10.1142/S1793984412400053

08/13/2012 3.00 Fengyu Li, Zhongfang Chen, Yafei Li. Graphane/Fluorographene Bilayer: Considerable C–H···F–C Hydrogen Bonding and Effective Band Structure Engineering,
Journal of the American Chemical Society, (07 2012): 0. doi: 10.1021/ja3040416

08/13/2012 2.00 Dihua Wu, Zhen Zhou, Carlos R. Cabrera, Yafei Li, Zhongfang Chen. Enhanced Li Adsorption and Diffusion on MoS,
The Journal of Physical Chemistry Letters, (08 2012): 0. doi: 10.1021/jz300792n

08/14/2014 26.00 Qing Tang, Jie Bao, Yafei Li, Zhen Zhou, Zhongfang Chen. Tuning band gaps of BN nanosheets and nanoribbons via interfacial dihalogen bonding and external electric field,
Nanoscale, (05 2014): 0. doi: 10.1039/C4NR00008K

08/14/2014 27.00 Zhongfang Chen, Yafei Li. Tuning Electronic Properties of Germanane Layers by External Electric Field and Biaxial Tensile Strain: A Computational Study,
The Journal of Physical Chemistry C, (01 2014): 0. doi: 10.1021/jp411783q

08/14/2014 28.00 Yu Jing, Zhen Zhou, Carlos R. Cabrera, Zhongfang Chen. Metallic VS2 Monolayer: A Promising 2D Anode Material for Lithium Ion Batteries,
The Journal of Physical Chemistry C, (12 2013): 0. doi: 10.1021/jp410969u

08/14/2014 29.00 Yafei Li, Yunlong Liao, Paul von Ragué Schleyer, Zhongfang Chen. Al2C monolayer: the planar tetracoordinate carbon global minimum,
Nanoscale, (07 2014): 0. doi: 10.1039/C4NR01972E

08/14/2014 30.00 Yafei Li, Yunlong Liao, Zhongfang Chen. Be2C Monolayer with Quasi-Planar Hexacoordinate Carbons:A Global Minimum Structure,
Angewandte Chemie International Edition, (07 2014): 0. doi: 10.1002/anie.201403833

08/14/2014 31.00 Yunlong Liao, Zhongfang Chen, John W. Connell, Catharine C. Fay, Cheol Park, Jae-Woo Kim, Yi Lin. Chemical Sharpening, Shortening, and Unzipping of Boron Nitride Nanotubes,
Advanced Functional Materials, (07 2014): 0. doi: 10.1002/adfm.201400599

08/14/2014 32.00 Yafei Li, Bay Allen Pantoja, Zhongfang Chen. Self-modulated Band Structure Engineering in C4F Nanosheets: First-Principles Insights,
Journal of Chemical Theory and Computation, (03 2014): 0. doi: 10.1021/ct401083c

08/14/2014 33.00 Xin Tan, Peng Jin, Zhongfang Chen. With the same Clar formulas, do the two-dimensional sandwich nanostructures X–Cr–X (X = C4H, NC3 and BC3) behave similarly?,
Physical Chemistry Chemical Physics, (2014): 0. doi: 10.1039/c3cp54838d

08/14/2014 34.00 Hongjun Liu, Zhongfang Chen, Sheng Dai, De-en Jiang. Selectivity trend of gas separation through nanoporous graphene,
Journal of Solid State Chemistry, (01 2014): 0. doi: 10.1016/j.jssc.2014.01.030

08/14/2014 35.00 Zhongfang Chen, Suvranu De, Qing Peng. A density functional theory study of the mechanical properties of graphane with van der Waals corrections,
Mechanics of Advanced Materials and Structures, (06 2014): 0. doi: 10.1080/15376494.2013.839067

08/14/2014 36.00 Yu Jing, Zhen Zhou, Carlos R. Cabrera, Zhongfang Chen. Graphene, inorganic graphene analogs and their composites for lithium ion batteries,
Journal of Materials Chemistry A, (05 2014): 0. doi: 10.1039/C4TA01033G

08/14/2014 37.00 Bin Chen, Zhenxing Fang, Yongfan Zhang, Zhongfang Chen, Kaining Ding. Why the photocatalytic activity of Mo-doped BiVO4 is enhanced: a comprehensive density functional study,
Physical Chemistry Chemical Physics, (2014): 0. doi: 10.1039/c4cp01350f

08/14/2014 39.00 Liang-Xing Wang, Chang-Gong Li, Fengyu Li, Zhongfang Chen, Li-Cheng Song. Synthetic and structural study on some new porphyrin or metalloporphyrin macrocycle-containing model complexes for the active site of [FeFe]-hydrogenases,
Journal of Organometallic Chemistry, (1 2014): 0. doi: 10.1016/j.jorganchem.2013.09.007

08/14/2014 40.00 Fengyu Li, De-en Jiang, Zhongfang Chen. Computational quest for spherical C12B68 fullerenes with “magic” pi-electrons and quasi-planar tetra-coordinated carbon,
Journal of Molecular Modeling, (02 2014): 0. doi: 10.1007/s00894-014-2085-z

08/14/2014 41.00 Chengchun Tang, Zhongfang Chen, Peng Jin. Carbon atoms trapped in cages: Metal carbide clusterfullerenes,
Coordination Chemistry Reviews, (07 2014): 0. doi: 10.1016/j.ccr.2013.10.020

08/14/2014 42.00 Kaining Ding, Bin Chen, Yulu Li, Yongfan Zhang, Zhongfang Chen. Comparative density functional theory study on the electronic and optical properties of BiMO4 (M = V, Nb, Ta),
Journal of Materials Chemistry A, (2014): 0. doi: 10.1039/c3ta15367c

08/29/2015 43.00 Shengli Zhang, Zhong Yan, Yafei Li, Zhongfang Chen, Haibo Zeng. Atomically Thin Arsenene and Antimonene: Semimetal-Semiconductor and Indirect-Direct Band-Gap Transitions,
Angewandte Chemie International Edition, (03 2015): 0. doi: 10.1002/anie.201411246

08/29/2015 44.00 Xin Tan, Fengyu Li, Zhongfang Chen. Metallic BSi3 Silicene and Its One-Dimensional Derivatives Unusual Nanomaterials with Planar Aromatic D6h Six-Membered Silicon Rings,
The Journal of Physical Chemistry C, (11 2014): 0. doi: 10.1021/jp507011p

08/29/2015 45.00 Fengyu Li, Kaixiong Tu, Zhongfang Chen. Versatile Electronic Properties of VSe2 Bulk, Few-Layers, Monolayer, Nanoribbons, and Nanotubes: A Computational Exploration,
The Journal of Physical Chemistry C, (09 2014): 0. doi: 10.1021/jp507093t

08/29/2015 48.00 Qing Peng, Liang Han, Xiaodong Wen, Sheng Liu, Zhongfang Chen, Jie Lian, Suvranu De. Mechanical properties and stabilities of ?-boron monolayers,
Phys. Chem. Chem. Phys., (2015): 0. doi: 10.1039/C4CP04050C

08/29/2015 46.00 Yu Wang, Yafei Li, Zhongfang Chen. Reducing Band Gap and Enhancing Carrier Mobility of Boron Nitride Nanoribbons by Conjugated ? Edge States,
The Journal of Physical Chemistry C, (10 2014): 0. doi: 10.1021/jp5078328

08/29/2015 47.00 Liang Han, Xiaodong Wen, Sheng Liu, Zhongfang Chen, Jie Lian, Suvranu De, Qing Peng. Mechanical properties and stabilities of g-ZnS monolayers,
RSC Adv., (01 2015): 0. doi: 10.1039/C4RA13872D

08/29/2015 49.00 Fengyu Li, Carlos R. Cabrera, Zhongfang Chen. Theoretical design of MoO3-based high-rate lithium ion battery electrodes: the effect of dimensionality reduction,
J. Mater. Chem. A, (09 2014): 0. doi: 10.1039/C4TA04340E

08/29/2015 50.00 Xin Tan, Carlos R. Cabrera, Zhongfang Chen. Metallic BSi3 Silicene: A Promising High Capacity Anode Material for Lithium-Ion Batteries,
The Journal of Physical Chemistry C, (11 2014): 0. doi: 10.1021/jp503597n

08/29/2015 51.00 Yu Wang, Hao Yuan, Yafei Li, Zhongfang Chen. Two-dimensional iron-phthalocyanine (Fe-Pc) monolayer as a promising single-atom-catalyst for oxygen reduction reaction: a computational study,
Nanoscale, (2015): 0. doi: 10.1039/C5NR00302D

08/29/2015 52.00 Xiaogang Han, Michael R. Funk, Fei Shen, Yu-Chen Chen, Yuanyuan Li, Caroline J. Campbell, Jiaqi Dai, Xiaofeng Yang, Jae-Woo Kim, Yunlong Liao, John W. Connell, Veronica Barone, Zhongfang Chen, Yi Lin, Liangbing Hu. Scalable Holey Graphene Synthesis and Dense Electrode Fabrication toward High-Performance Ultracapacitors,
ACS Nano, (08 2014): 0. doi: 10.1021/nn502635y

08/29/2015 53.00 Li-Ming Yang, Eric Ganz, Zhongfang Chen, Zhi-Xiang Wang, Paul von Ragué Schleyer. Four Decades of the Chemistry of Planar Hypercoordinate Compounds,
Angewandte Chemie International Edition, (08 2015): 0. doi: 10.1002/anie.201410407

08/29/2015 54.00 Juanyuan Hao, Fengyu Li, Hongjiang Li, Xiaoyu Chen, Yuyan Zhang, Zhongfang Chen, Ce Hao. Dynamic motion of an Lu pair inside a C76(Td) Cage ,
RSC Adv., (2015): 0. doi: 10.1039/C4RA16236F

08/29/2015 55.00 Peng Jin, Qinghua Hou, Chengchun Tang, Zhongfang Chen. Computational investigation on the endohedral borofullerenes M@B40 (M = Sc, Y, La),
Theoretical Chemistry Accounts, (1 2015): 0. doi: 10.1007/s00214-014-1612-4

08/29/2015 56.00 Xiaoming Huang, Jijun Zhao, Yan Su, Zhongfang Chen, R. Bruce King. Design of Three-shell Icosahedral Matryoshka Clusters A@B12@A20 (A = Sn, Pb; B = Mg, Zn, Cd, Mn),
Scientific Reports, (11 2014): 0. doi: 10.1038/srep06915

08/29/2015 57.00 Jijun Zhao, Xiaoming Huang, Peng Jin, Zhongfang Chen. Magnetic properties of atomic clusters and endohedral metallofullerenes,
Coordination Chemistry Reviews, (04 2015): 0. doi: 10.1016/j.ccr.2014.12.013

TOTAL: **63**

Number of Papers published in peer-reviewed journals:

(b) Papers published in non-peer-reviewed journals (N/A for none)

Received Paper

05/20/2016 76.00 Fengyu Li, Peng Jin, Yunlong Liao , Zhongfang Chen, Jiacheng Feng. SEARCHING FOR NEW MEMBERS OF C70HOMOFULLERENES BY FIRST-PRINCIPLESCOMPUTATIONS: BENT'S RULE AT WORKON C70 SURFACE,
Journal of Theoretical and Computational Chemistry, (02 2013): 1250097. doi:

TOTAL: **1**

Number of Papers published in non peer-reviewed journals:

(c) Presentations

Number of Presentations: 0.00

Non Peer-Reviewed Conference Proceeding publications (other than abstracts):

Received	Paper

TOTAL:

Number of Non Peer-Reviewed Conference Proceeding publications (other than abstracts):

Peer-Reviewed Conference Proceeding publications (other than abstracts):

Received	Paper
05/24/2013 9.00	Fengyu Li, Zhongfang Chen. Lithium Adsorption and Diffusion in MoO3 bulk and on MoO3 Monolayer: A Computational Investigation , ACS Spring Meeting, Energy & Fuels Division. 07-APR-13, . : ,

TOTAL: **1**

Number of Peer-Reviewed Conference Proceeding publications (other than abstracts):

(d) Manuscripts

Received	Paper
05/20/2016 59.00	Yunlong Liao, Wei Cao, John W. Connell, Zhongfang Chen, Yi Lin. Evolution of Moiré Profiles from van der Waals Superstructures of Boron Nitride Nanosheets, Scientific Reports (03 2016)
08/13/2012 4.00	. Searching For New Members of C70 Homofullerenes by First-Principles Computations: Bent's Rule at Work on C70 Surface, Journal of Computational and Theoretical Chemistry (05 2012)
08/13/2012 5.00	. Is C60 Buckminsterfullerene Aromatic?, Phys. Chem. Chem. Phys. (06 2012)

TOTAL: **3**

Number of Manuscripts:

Books

Received	Book
08/12/2013	20.00 . Graphene Chemistry: Theoretical Perspectives, : , ( )
08/12/2013	21.00 . Book chapter, Introduction, in Book chapter in Graphene Chemistry: Theoretical Perspectives, edited by De-en Jiang and Zhongfang Chen, John Wiley & Sons, 2013, : , ( )
08/12/2013	22.00 . Book chapter, Understanding Aromaticity of Graphene and Graphene Nanoribbons by Clar Sextet Rule, Book chapter in Graphene Chemistry: Theoretical Perspectives, edited by De-en Jiang and Zhongfang Chen, John Wiley & Sons, 2013, Chapter 3, : , ( )
08/12/2013	23.00 . Book chapter, in Graphene Chemistry: Theoretical Perspectives, edited by De-en Jiang and Zhongfang Chen, John Wiley & Sons, 2013, Chapter 13, : , ( )
08/12/2013	24.00 . Book chapter, Graphene-Based Materials as Nanocatalysts, Book chapter in Graphene Chemistry: Theoretical Perspectives, edited by De-en Jiang and Zhongfang Chen, John Wiley & Sons, 2013, Chapter 15, : , ( )
08/12/2013	25.00 . Book chapter, Hydrogen Storage in Graphene, Book chapter in Graphene Chemistry: Theoretical Perspectives, edited by De-en Jiang and Zhongfang Chen, John Wiley & Sons, 2013, Chapter 16, : , ( )

TOTAL: **6**

Received	Book Chapter

TOTAL:

Patents Submitted

Patents Awarded

Awards

Graduate Students

NAME	PERCENT_SUPPORTED	Discipline
Yunlong Liao	1.00	
Kaixiong Tu	0.08	
Fuzhao Yi	0.00	
Si Yang	0.00	
Ya Wang	0.00	
FTE Equivalent:	**1.08**	
Total Number:	**5**	

Names of Post Doctorates

NAME	PERCENT_SUPPORTED
Jingxiang Zhao	0.00
Haijun Zhang	0.00
Jianhua Huo	0.00
FTE Equivalent:	**0.00**
Total Number:	**3**

Names of Faculty Supported

NAME	PERCENT_SUPPORTED
FTE Equivalent:	
Total Number:	

Names of Under Graduate students supported

NAME	PERCENT_SUPPORTED	Discipline
Gabriel Reilly	0.00	Computer and Computational Sciences
FTE Equivalent:	**0.00**	
Total Number:	**1**	

Student Metrics

This section only applies to graduating undergraduates supported by this agreement in this reporting period

The number of undergraduates funded by this agreement who graduated during this period: 0.00

The number of undergraduates funded by this agreement who graduated during this period with a degree in science, mathematics, engineering, or technology fields:..... 1.00

The number of undergraduates funded by your agreement who graduated during this period and will continue to pursue a graduate or Ph.D. degree in science, mathematics, engineering, or technology fields:..... 1.00

Number of graduating undergraduates who achieved a 3.5 GPA to 4.0 (4.0 max scale):..... 1.00

Number of graduating undergraduates funded by a DoD funded Center of Excellence grant for Education, Research and Engineering:..... 0.00

The number of undergraduates funded by your agreement who graduated during this period and intend to work for the Department of Defense 1.00

The number of undergraduates funded by your agreement who graduated during this period and will receive scholarships or fellowships for further studies in science, mathematics, engineering or technology fields:..... 0.00

Names of Personnel receiving masters degrees

NAME

Total Number:

Names of personnel receiving PHDs

NAME

Total Number:

Names of other research staff

NAME PERCENT_SUPPORTED

FTE Equivalent:
Total Number:

Sub Contractors (DD882)

Inventions (DD882)

Scientific Progress

See Attachment.

Technology Transfer

Progress Reports

Theory-guided Innovation of Noncarbon Two-dimensional Nanomaterials,
DoD (W911NF-12-1-0083, February 15, 2015-February 14, 2016)

Professor Zhongfang Chen
Department of Chemistry
University of Puerto Rico
San Juan, PR 00931

We have investigated two-dimensional (2D) nanomaterials, especially those made of non-carbon elements, elucidated their intrinsic properties, and explored their applications in nanoelectronics and energy-related applications by means of larger-scale density functional theory (DFT) computations, carried out experiments guided by our computations. Moreover, we have also theoretically addressed some important questions in nanochemistry,

1. Theoretical studies of novel non-carbon 2D nanomaterials and their derivatives

By means of comprehensive and systematic DFT computations, we computationally designed novel 2D nanomaterials with unique structures and exceptional properties, such as functionalized boron nitride, molybdenum disulfide (MoS_2), molybdenum oxide (MoO_3), Al_2C monolayer with planar tetracoordinate carbon, Be_2C monolayer with quai-planar hexacoordiate carbon, Be_5C_2 monolayer with quasi-planaer pentacoordinate carbon, FeB_6 monolayers hypercoordinate transition metal, semiconducting Group 15 monolayers, bismuth iodide monolayers, PdS_2 monolayers with unprecedented structure as other transition-metal disulfides, pentagonal B_2C Monolayer, explore new approaches to tune their electronic, magnetic and mechanical properties, examined their potential applications of 2D materials in nanoelectronics and mechanics, and identified promising materials as lithium ion battery electrodes, anchoring materials for lithium-sulfur batteries, nanocatalysts for oxygen reduction reaction in fuel cells, and gas separation membranes.

1.1. 2D nanomaterials with rule-breaking chemical bonding

Designing new materials is always desirable for the promise of new properties and applications, and it is particular interesting when the material contains some peculiar topological properties, such as reduced dimensionality and rule-breaking chemical bonding.

Along this route, we first designed a novel 2D inorganic material, namely Al_2C monolayer, and its one-dimensional nanoribbons. In Al_2C monolayer, each carbon atom binds to four Al atoms in an exact plane, forming a planar tetracoordinate carbon (ptC) moiety, which has intrigued the chemistry community for decades. Our computations reveal that Al_2C monolayer has good stability, and is the lowest-energy

structure in the 2D space. Moreover, Al_2C monolayer is semiconducting with a moderate band gap, which is promising for wide applications in electronics and optoelectronics. Cutting 2D Al_2C monolayer into Al_2C nanoribbons can result in quite rich characteristics: they can have a direct or indirect band gap with different values, depending on the cutting direction and edge configuration. These results have been published in *Nanoscale*, **2014,** 6, 10784.[1]

We further designed a novel 2D inorganic material, namely Be_2C monolayer, in which each carbon atom binds to six Be atoms on the nearly same plane, forming a quasi planar hexacoordinate carbon (phC) moiety, the notion of which was proposed by Schleyer et al. at the beginning of this century. Our computations reveal that Be_2C monolayer has good stability, as indicated by its moderate cohesive energy, high in-plane stiffness, absence of imaginary phonon modes, and high melting point. Especially, the phC-containing Be_2C monolayer is the lowest-energy structure in the 2D space, confirmed by a global minima search based on the particle-swarm optimization (PSO) method. Moreover, Be_2C monolayer is also semiconducting with a moderate direct band gap, which is promising for wide applications in electronics and optoelectronics. These results have been publishd in *Angew. Chem. Int. Ed*. **2014**, *53*, 7248.[2]

Recently, we designed a new two-dimensional material, namely Be_5C_2 monolayer on the basis of DFT computations. In Be_5C_2 monolayer, each carbon atom binds with five beryllium atoms in the almost same plane, forming a quasi-planar pentacoordinate carbon moiety. Be_5C_2 monolayer has good stability, as revealed by its moderate cohesive energy, positive phonon modes, and high melting point. Especially, it is the lowest-energy structure with the Be_5C_2 stoichiometry in two-dimensional space, thus holds great promise to be realized experimentally. Remarkably, Be_5C_2 monolayer is a gapless semiconductor with a Dirac-like point in the band structure, and also has an unusual negative Poisson's ratio. Once synthesized, Be_5C_2 monolayer may find many applications in electronics and mechanics. These results have been published in *Nature Communications*, **2016**, *7*, 11488.[3]

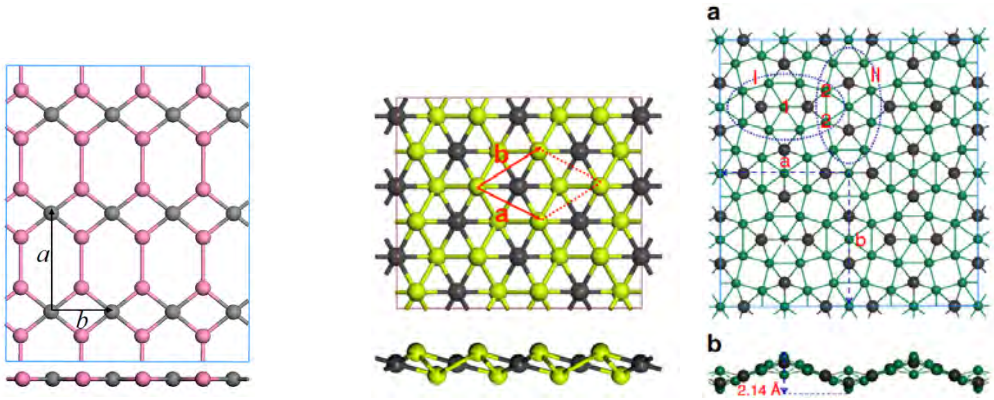

Figure 1. Top (upper) and side (lower) views of geometric structure of 2D Al_2C monolayer (left), Be_2C monolayer (middle) and Be_5C_2 monolayer.

By means of DFT computations and global minimum search using particle-swarm optimization (PSO) method, we predicted three FeB_6 monolayers, namely α-FeB_6, β-FeB_6 and γ-FeB_6, which consist of the Fe©B_x (x = 6, 8) wheels with planar hypercoordinate Fe atoms locating at the center of six- or eight-membered boron rings. In particular, the α-FeB_6 sheet constructed by Fe©B_8 motifs is the global minimum due to completely shared and well delocalized electrons. The two-dimensional (2D) boron networks are dramatically stabilized by the electron transfer from Fe atoms, and the FeB_6 monolayers have pronounced stabilities. The α-FeB_6 monolayer is metallic, while the β-FeB_6 and γ-FeB_6 sheets are semiconductors with indirect band gaps and significant visible-light absorptions. Besides the novel chemical bonding, the high feasibility for experimental realization, and unique electronic and optical properties, render them very welcome new members to the graphene-like materials family. These results have been published in *J. Am. Chem. Soc.* **2016**, *138*, 5644–5651.[4]

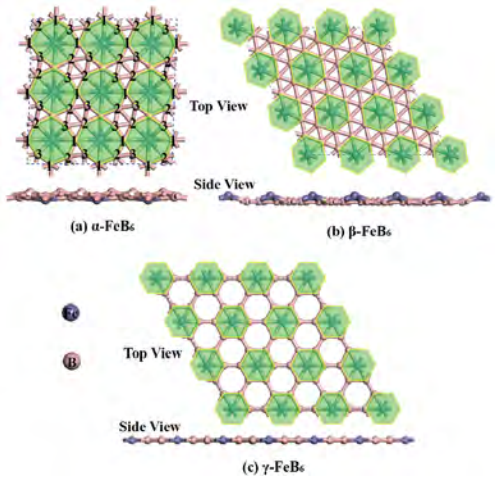

Figure 2. Optimized geometries of α-FeB_6, β-FeB_6 and γ-FeB_6 monolayers. Green-filled octagons and hexagons are guidelines for Fe©B_8 and Fe©B_6 wheels, respectively.

These four papers are among the first attempts to extend the planar hypercoordination carbon/transition metal concept to 2D monolayers, and would greatly enrich our basic knowledge on chemical bonding and inspire more theoretical efforts on designing materials with novel chemical bonding. Moreover, our predicted structures are global minima on the 2D space and have some quite promising applications. Our work would motivate the experimental peers to realize them in the laboratory, just similar to the cases of graphene and silicene. My group is trying to collaborate with peers to achieve such exciting materials.

1.2. Emerging 2-D nanomaterials with unique structures and exceptional properties

1.2.1. Atomically Thin Arsenene and Antimonene

The typical two-dimensional (2D) semiconductors of MoS_2, $MoSe_2$, WS_2, WSe_2 and black P have garnered tremendous interest for their unique electronic, optical and chemical properties. However, 2D semiconductors are still so limited that all bandgaps are below 2.0 eV, which have greatly restricted their applications, especially in optoelectronic devices with photoresponse in the blue and UV wave bands.

We investigated novel 2D mono-elemental semiconductors, monolayered arsenene and antimonene, with both wide bandgaps and high stability. Interestingly, although As and Sb bulks are typical semimetals, they are transformed into indirect semiconductors with band gaps of 2.49 and 2.28 eV when thinned into one atomic layer. Significantly, further loading of tiny biaxial strain can transform them from indirect into direct band-gap semiconductors. Such dramatic electronic structure transitions could open a new door for transistors with high on/off ratio, blue/UV optoelectronic devices, and mechanical sensors based on new 2D crystals. These results have been published in *Angew. Chem. Int. Ed.* **2015**, *54*, 3112-3115.[5] Our finding was highlighted by Nature as a Research Highlight (*Nature* 2015, 517, 246).

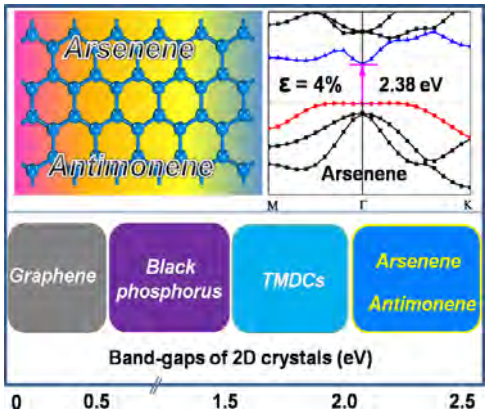

Figure 3. Schematic structure of arsenene/antimonene, the effect of biaxial strain to the band structure of arsenene, and the band gaps of arsenene/antimonene

1.2.2. Semiconducting Group 15 monolayers

Optoelectronic applications require materials both responsive to objective photons and able to transfer carriers, so new 2D semiconductors with appropriate bandgaps and high mobilities are highly desired. Here, we report on the attractive broadband gap and high mobility of a 2D semiconductor family, composed of monolayer of group-V elements (phosphorene, arsenene, antimonene and bismuthene). The calculated binding energies and phonon band dispersions of 2D group-V allotropes exhibit energetic and kinetic stability. 2D semiconducting group-V monolayers own versatile energy bandgaps from 0.36 to 2.62 eV, which are helpful for broadband photoresponse. Significantly, phosphorene, arsenene and bismuthene possess carrier mobilities as high as several thousand $cm^2 \cdot V^{-1} \cdot s^{-1}$. Combining such

broadband gaps and superior carrier mobilities, 2D Vgroup-V monolayers are promising candidates for nanoelectronics and optoelectronics. These results have been published in *Angew. Chem. Int. Ed.* **2016**, *55*, 1666-1669.[6]

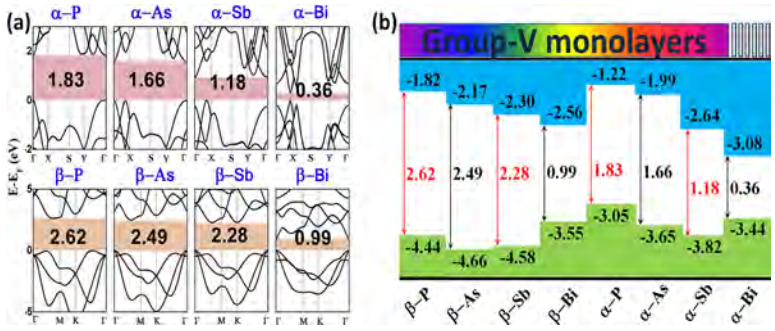

Figure 4. a) Electronic band structures of group-V monolayers at the HSE06 level of theory, b) Energy levels of group-V monolayers calculated also at the HSE06 level of theory, which indicate that group-V monolayers can own broadband photoresponse.

1.2.3. Single-layer bismuth iodide (BiI_3)

By means of DFT computations, we investigated in detail the structural, electronic, mechanical and optical properties of the single-layer bismuth iodide (BiI_3) nanosheet. Monolayer BiI_3 is dynamically stable as confirmed by the computed phonon spectrum. The cleavage energy and interlayer coupling strength of bulk BiI_3 are comparable to the experimental values of graphite, which indicates that the exfoliation of BiI_3 is highly feasible. The obtained stress-strain curve shows that the BiI_3 nanosheet is a brittle material with a breaking strain of 13%. The BiI_3 monolayer has an indirect band gap of 1.57 eV with spin orbit coupling (SOC), indicating its potential application for solar cells. Furthermore, the band gap of BiI_3 monolayer can be modulated by biaxial strain. Most interestingly, interfacing electrically active graphene with monolayer BiI_3 nanosheet leads to enhanced light absorption compared to that in pure monolayer BiI_3 nanosheet, highlighting its great potential applications in photonics and photovoltaic solar cells. These results have been published in *Scientific Reports*, **2015**, *5*, 17558.[7]

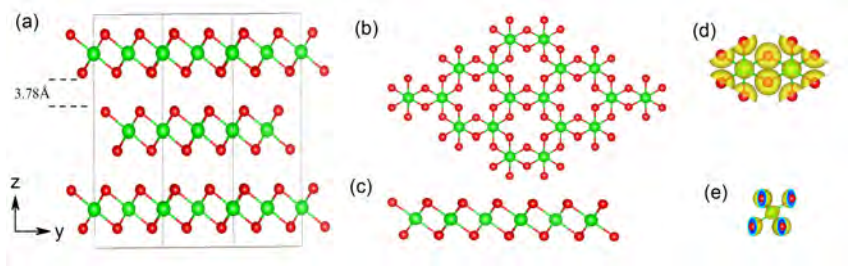

Figure 5. (a) Side view of BiI_3 bulk crystal; (b) top and (c) side views of BiI_3 nanosheet; red and green ball represent the iodine and bismuth atoms, respectively; (d) top and (e) side views of Iso-surface (0.045 ev/au^3) for electronic density of monolayer BiI_3.

1.2.4. 2D transition-metal disulfides with unprecedented structure: PdS_2 monolayer

Two dimensional (2D) transition-metal disulfides (TMDs) nanostructures, such as single-layered MoS_2, WS_2, and TiS_2, are emerging materials for nano-electronics as they exhibit unique properties complementary or even surpassing those of graphene, such as a sizeable band gap.

By means of DFT computations, we investigated the structural and electronic properties of a novel 2D-TMD, named PdS_2 monolayer. Distinguished from other 2D TMDs which adopt the ordinary 2H or 1T configuration, PdS_2 monolayer presents rather unique structural properties: each Pd atom binds to four S atoms in the same plane, and two neighboring S atoms can form a covalent S–S bond. The hybrid HSE06 DFT computations demonstrated that PdS_2 monolayer is semiconducting with an indirect band gap of 2.08 eV, which can be effectively reduced by employing a uniaxial or biaxial tensile strain. Especially, PdS_2 has a rather large hole and electron mobilities. Our results suggest that PdS_2 monolayer is rather promising for future electronics and optoelectronics. These results have been published in *J. Mater. Chem. C.* **2015**, *3*, 9603.[8]

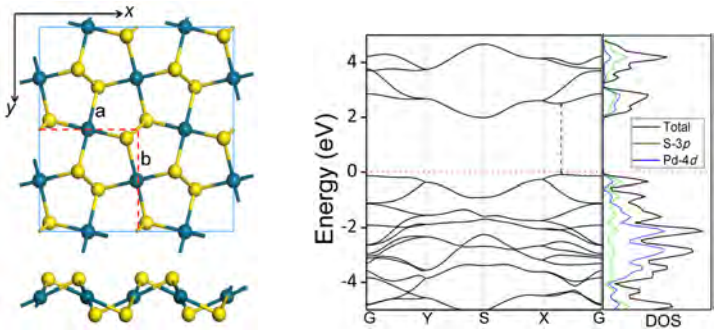

(a) (b)

Figure 6. (a) Top (upper) and side (bottom) views of the PdS_2 monolayer. Black green and yellow balls represent Pd and S atoms, respectively. (b) Band structure (left) and density of states (right) of PdS_2 monolayer. The red dashed line denotes the position of Fermi level while the blue double arrow denotes the direct band gap.

1.2.5. Flexible structural and electronic properties of pentagonal B_2C monolayer via external strain

Inspired by the recent theoretical finding that penta-graphene, composed entirely of carbon pentagons, is dynamically and mechanically stable [*PNAS*, 2015, 112, 2372–2377.], we computationally designed a new two-dimensional (2D) inorganic material, a pentagonal B_2C monolayer (penta-B_2C), in which each pentagon contains three boron and two carbon atoms, the C is four-coordinated with four B atoms, and all the B atoms are three-coordinated with two C and one B, forming a buckled 2D network. The pentagonal B_2C monolayer is semiconducting with a wide indirect band gap of 2.28 eV from HSE calculation. The absence of imaginary modes in its phonon spectrum, and the high melting point predicted by molecular dynamics (MD)

simulations indicate its good persistence. Interestingly, the buckled structure could be stretched to planar under 15% biaxial tensile, and the band gap will be strikingly reduced to 0.06 eV. The semiconducting penta-B_2C could also be switched to a metal under certain biaxial strains, while uniaxial strains can only tune the band gaps without changing the semiconducting character. As a novel type of 2D inorganic material, the good persistence of penta-B_2C offers us a new clue to design 2D inorganic materials with unusual structural and electronic properties. These results have been published in *Phys. Chem. Chem. Phys*. **2015**, 17, 24151.[9]

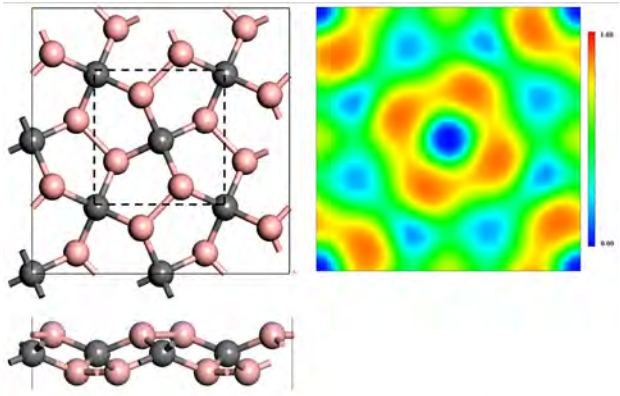

(a) (b)

Figure 7. (a) Top and side views of the optimized penta-B_2C monolayer. The dashed square denotes the unitcell. (b) Deformation charge density of the 2D penta-B_2C monolayer.

1.2.6. Metallic BSi_3 silicene and its one-dimensional derivatives

Achieving 2D aromatic compounds with planar cyclic six-membered silicon rings (c-Si_6) is a grand challenge. By means of density functional theory (DFT) computations, we predicted that c-BSi_3 silicene, the global minimum of BSi_3 monolayer, contains planar aromatic D_{6h} c-Si_6. In c-BSi_3 silicene, the strong π-p conjugation between c-Si_6 and B atoms is responsible for the planar geometry of the aromatic D_{6h} c-Si_6, which is in stark contrast to the conventional bonding motifs of silicon (sp^3-bonding).

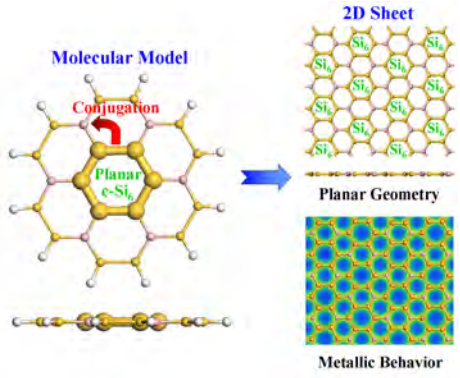

Figure 8. The structure of BSi_3 monolayer and its so-surface of deformation electronic density

Interestingly, the 2D c-BSi_3 silicene and its one-dimensional (1D) derivatives (c-BSi_3 nanotubes and nanoribbons) are metallic, regardless of the charity, tube diameter, or ribbon width, and the metallic behavior of c-BSi_3 silicene is very robust to mechanical strain and surface chemical functionlization. The high stabilities of these systems strongly suggest the feasibility for their experimental realizations. These results have been published in *J. Phys. Chem. C.* **2014**, *118*, 25825,[10] which was highlighted as a journal cover.

1.2.7. VSe_2 few-layers, monolayer, nanoribbons, and nanotubes

We investigated the stabilities, magnetic and electronic properties of VSe_2 bulk, few-layer, monolayer, and its derived nanoribbons (NRs) and nanotubes in both T and H phases. All these materials are ferromagnetic, but exhibit versatile electronic properties. The VSe_2 bulk and few-layers in either T or H phase, and T-monolayer are metallic, while the T-monolayer is a semiconductor. For nanoribbons, the zigzag NRs in both T- and H phases and the armchair NRs in T-phase are metallic, while the armchair NRs in H-phase are half-metallic. The edge hydrogenation can retain or amend the electronic property of the pristine NRs depending on the charality and phases. Regardless of the chirality, nanotubes in T phase are half-metallic, while those in H phase are metals. These findings provide a simple and effective route to tune the electronic properties of VSe_2 nanostructures in a wide range and also facilitate the design of VSe_2-based nanodevices. These results have been published in *J. Phys. Chem. C.* **2014**, *118*, 21264.[11]

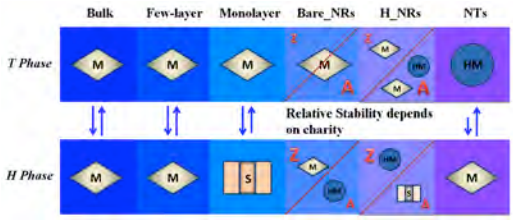

Figure 9. The magnetic and electronic properties of VSe_2 bulk, few-layers, monolayer and nanoribbons with different phases

1.3. New methods to modulate electronic and magnetic structures of 2D materials

1.3.1. Tuning electronic structure of bilayer MoS_2 by vertical electric field

The bandgaps of the bilayer MoS_2 monotonically decrease with an increasing vertical electric field. The critical electric fields, at which the semiconductor-to-metal transition occurs, are predicted to be in the range of 1.0−1.5 V/Å depending on different stacked conformations. These results have been published in *J. Phys. Chem. C.* **2012**, *116*, 21556.[12]

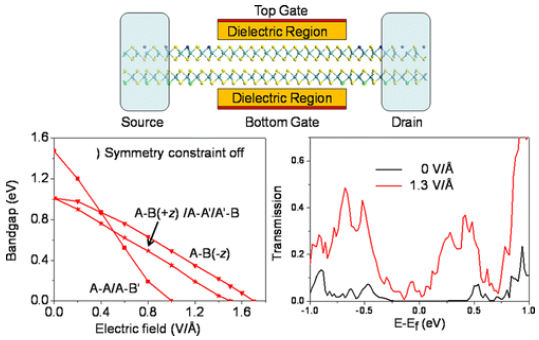

Figure 10. Tuning electronic sructure of bilayer MoS_2 by vertical electric field

1.3.2. Tuning electronic properties of germanane layers by external electric field and biaxial tensile strain

We demonstrated that germanane monolayer, a newly synthesized 2D material is semiconducting with a moderate direct band gap (1.5 eV). Germanane monolayers can be stacked together via the strong interlayer hydrogen bonding. Especially, germanane layers all have a direct band gap, irrespective of the stacking pattern and the thickness, which is a big advantage over MoS_2 layers. Moreover, considering that the controllable band gap engineering is always desirable for a wide range of applications, we proposed theoretically two approaches, namely external electronic field and biaxial tensile strain, towards tuning the electronic properties of germanane layers. It was found that the band gap of germanane bilayer can be flexibly reduced by applying an external electronic field (E-field), leading to a semiconducting-metallic transition, whereas the band gap of germanane monolayer is rather robust in response to E-field. In contrast, the band gaps of both germanane monolayer and bilayer can be reduced to zero when subjected to a biaxial tensile strain. These results would promote the applications of germanane layers in optoelectronics and have been published in *J. Phys. Chem. C*, **2014**, *118*, 1148. [13]

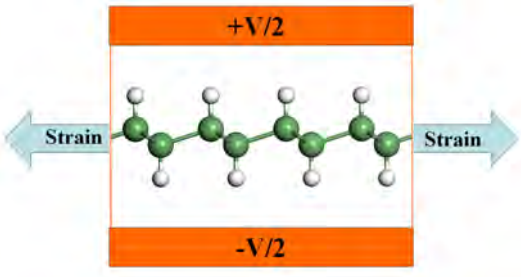

Figure 11. The electronic properties of germanane layers can be tuned by external electric field and biaxial tensile strain.

1.3.3. Tuning Electronic and Magnetic Properties of MoO_3 Sheets by Cutting, Hydrogenation, and External Strain

The electronic and magnetic properties of MoO_3 nanosheets can be effectively tuned in a wide range by cutting into nanoribbons, hydrogenation and external strains. These findings provide a simple and effective route to tune the magnetic and

electronic properties of MoO_3 nanostructures in a wide range, and thus facilitate the design of MoO_3-based nanodevices. These results have been published in *Nanoscale*, **2013**, *5*, 5321.[14]

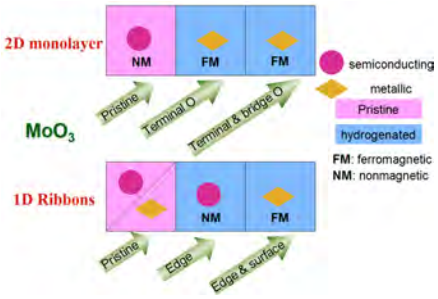

Figure 12. The electronic and magnetic properties of MoO_3 sheets can be tuned by cutting, hydrogenation, and external strain

1.3.4. Quantum spin Hall insulators in strain-modified arsenene

As new quantum states of matter, topological insulators (TIs) have recently attracted extensive research interest due to their bulk insulting gap and topologically protected boundary states. 2D TIs are considered as more promising materials than three-dmimensional (3D) TIs for spin transport applications because the edge states in the former are more robust against back-scattering than surface states in the latter. However, due to the weak spin-orbital coupling (SOC), the 2D QSH insulators have to overcome the deficiency of their small bulk gap and low-temperature operation.

By means of DFT computations, we predict that suitable strain modulation of honeycomb arsenene results in a unique 2D topological insulator (TI) with a sizable bulk gap (up to 696 meV), which could be characterized and utilized at a room temperature. Without considering any spin-orbital coupling, the band inversion occurs around Gamma (G) point at tensile strains larger 11.7%, which indicates the quantum spin Hall effect in arsenene at appropriate strains. The nontrivial topological phase was further confirmed by the topological invariant $\nu = 1$ and edge states with single Dirac-type crossing at G point. Our results provide a promising strategy for designing 2D TIs with large bulk gaps from the commonly used materials. These results have been published in *Nanoscale*, **2015**, *7*, 19152.[15]

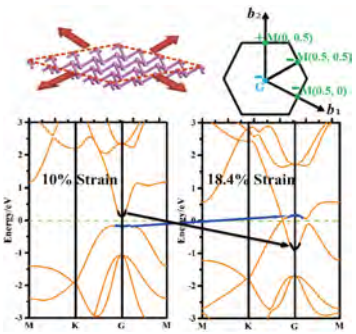

Figure 13. The quantum spin Hall effect in arsenene at appropriate strains.

1.3.5. New approaches to tune the band structure of BN nanoribbons

By means of DFT computations, we systematically examined the uniform bending effect on the electronic properties of armchair boron nitride nanoribbons (aBNNRs) with experimentally obtained width. For both bare and hydrogen-terminated aBNNRs, the band gaps only slightly depend on the uniform bending. The insensitivity of the band structures of BNNRs to the uniform bending makes them ideal materials when their wide band-gap character is desired. These results have been published in *Nano Life*, **2012**, 2, 1240005.[16]

The wide band gap of boron nitride (BN) materials has been a main bottleneck for their wide applications in electronics. We demonstrated that the band gaps of BN nanoribbons (BNNRs), with either zigzag or armchair edges, can be significantly reduced by C_2H termination. The neighboring C_2H terminal groups of BNNRs can covalently connect with each other, forming infinite carbon chains along the edges. The newly formed carbon chains introduce conjugated π edge states, which contribute to the band gap reduction of BNNRs. C_2H termination can also result in higher carrier mobility for BNNRs. This simple strategy offers great opportunities for developing BNNRs based electronic devices. These results have been published in *J. Phys. Chem. C.* **2014**, *118*, 25051.[17]

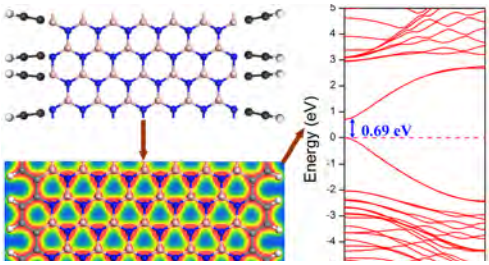

Figure 14. C_2H terminal groups can reduce the band gap and enhance carrier mobility of BN nanoribbons

1.3.5. Tuning the band structures of 2D nanomaterials by non-covalent interactions

A promising simple and effective, *yet not well-explored* method to tune the electronic structure of carbon graphene and other monolayer nanostructures is to employ weak interactions.

Graphane/Fluorographene Bilayer: Considerable C−H···F−C Hydrogen Bonding and Effective Band Structure Engineering

By means of DFT computations, we demonstrated theoretically that graphane and fluographene can be paired together through the C–H···F–C hydrogen bonds. The unique C–H···F–C bonds define the conformation of graphane/fluorographene (G/FG) bilayer and contribute to its stability. Interestingly, G/FG bilayer has an energy gap (0.5 eV) much lower than those of individual graphane and fluorographene. The

binding strength of G/FG bilayer can be significantly enhanced by applying appropriate external electric field (E-field). Especially, changing the direction and strength of E-field can effectively modulate the energy gap of G/FG bilayer, and correspondingly causes a semiconductor–metal transition. These results have been published in *J. Am. Chem. Soc.* **2012**, *134*,11269.[18]

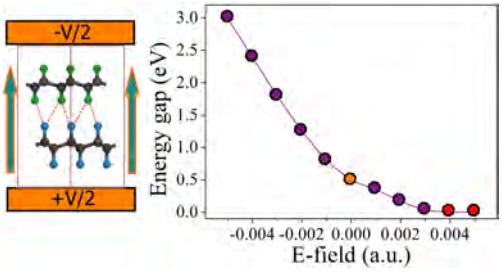

Figure 15. The band structure of G/FG bilayer tuned by the external electric field.

Self-modulated band structure engineering in C_4F nanosheets by dipole-dipole interactions

For the first time, we reveled that there are considerable $C^{\delta+}F^{\delta-}\cdots C^{\delta+}$ $F^{\delta-}$ dipole-dipole interactions between patterned partially fluorinated graphene (C_4F) monolayers, which were already experimentally realized. Especially, the dipole-dipole interactions induce a subtle interlayer polarization, which results in a significantly reduced band gap for C_4F bilayer compared with individual C_4F monolayer. With increasing the number of stacked layers, the band gap of C_4F nanosheets can be further reduced, leading to a semiconducting–metallic transition. Moreover, the band gap of C_4F nanosheets can be feasibly modulated by applying an external electric field. This study provides a rather practical method toward tuning the electronic properties of graphene materials, and will promote more efforts in using weak interactions to tune the band structures of graphene and related materials. These results have been published in *J. Chem. Theory Comput.* **2014,** *10*, 1265.[19]

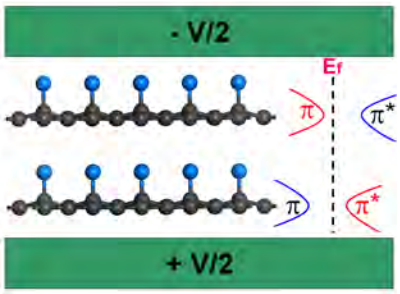

Figure 16. The band structure of C_4F nanosheets can be modulated by dipole-dipole interactions and applied external electric field.

XH/π (X = C, Si) intractions in graphene and silicene

Following the above mentioned work of using interlayer hydrogen bonds to tune the electronic band gaps of graphane/fluorinated graphene, we demonstrated that considerable CH/π interactions exist between graphene and its patterned partially (C_4H) hydrogenated derivatives, a 90 meV band gap is opened in graphene/C_4H bilayer, and this band gap can be further increased to 270 meV by sandwiching graphene between two C_4H layers. By taking advantage of the similar SiH/π interactions, a 120 meV band gap also can be opened for silicene. Interestingly, the high carrier mobility of graphene/silicene can be well preserved.[20]

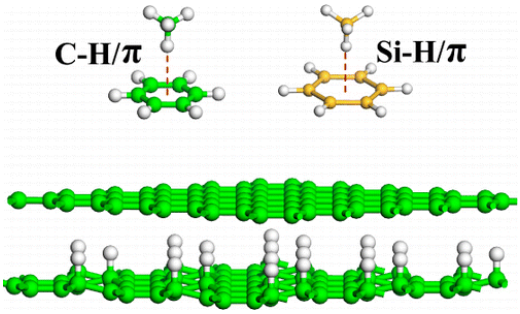

Figure 17. CH/π or SiH/π interactions can open a band gap in graphene and silicene

Band gap engineering of BN sheet by interlayer dihydrogen bonding and electric field control

The interlayer B-H···H-N dihydrogen bonds are established in the hydrogenated bilayer BN nanosheets. The presence of such bonding can drastically reduce the intrinsic large band gaps of chair-typed BN configuration (a meta-stable structure) due to interlayer charge transfer. While the insulating properties of the more stable stirrup-typed bilayer BN can be engineered by applying electric field. These fascinating results illuminate a new pathway for band engineering of 2D BN nanomaterials. These results have been published in *ChemPhysChem* **2013**, *14*, 1787.[21]

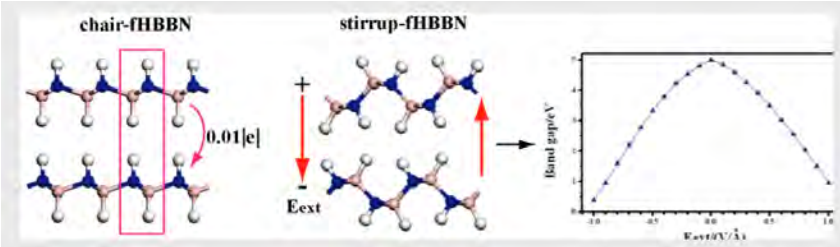

Figure 18. The BN naosheets can be stacked by dihydrogen bonds, and the band gap of BN nanosheets can be engineered by interlayer dihydrogen bonding and electric field control.

Tuning band gaps of BN nanosheets and nanoribbons via interfacial dihalogen bonding and external electric field

We performed systematic DFT computations to study the dihalogen interactions and their effect on band structures in halogenated (fluorinated and chlorinated) BN bilayers and the aligned halogen-passivated zigzag BN nanoribbons (BNNRs). Our findings are very intriguing: (1) Considerable homo-halogen (F···F and Cl···Cl) interactions exist in fluoro (chloro)-BN bilayer (aligned ribbons), and substantial hetero-halogen (F···Cl) interactions are available in hybrid fluor-BN/chloro-BN bilayer (aligned hybrid ribbons); (2) These dihalogen interactions at the 2D or 1D interfaces lead to significant band-gap reduction for the interactive BN nanosystems, and their binding strengths and electronic properties can be further controlled by applying an external electric field, wherein an extensive modulation from large- to medium-band-gap semiconductors, or even metals can be realized by simply adjusting the direction and strength of the applied electric field. This work offers insightful prospects to flexibly tune the large bandgap of BN nanosystems, which would facilitate the design and application of BN materials in next-generation nanoelectronic devices. These results have been published in *Nanoscale* **2014**, *6*, 8624.[22]

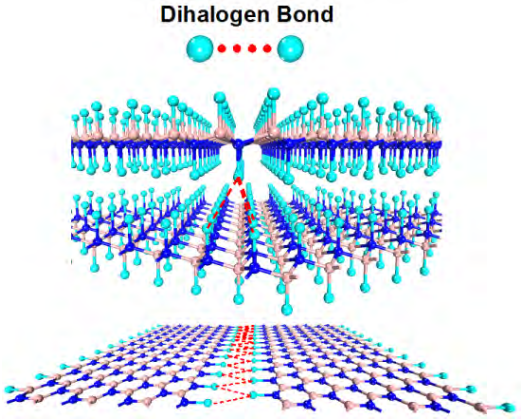

Figure 19. The BN naosheets can be stacked by dihalogen interactions, and the band gap of BN nanosheets and nanoribbons can be engineered by interlayer dihalogen bonding and electric field control.

Attaching a floating induced dipole field via π-π interactions to zigzag nanoribbons

We also identified a simple strategy to modulate the electronic and magnetic properties of zigzag graphene nanoribbons (zGNRs), which takes advantage of the effect of the floating dipole field attached to zGNRs via π -π interactions. By simply depositing the ladder-structure acceptor/donor-decorating PDA derivatives on zGNRs via strong π-π interactions, the abundant electronic and magnetic transformations, namely spin gapless semiconducting (SGS) – half-metallic – metallic transition, along with the magnetic conversion from antiferromagnetic to ferromagnetic, can be achieved in zGNRs. These results have been published in *Adv. Funct. Mater.* **2013**, *23*, 1507.[23]

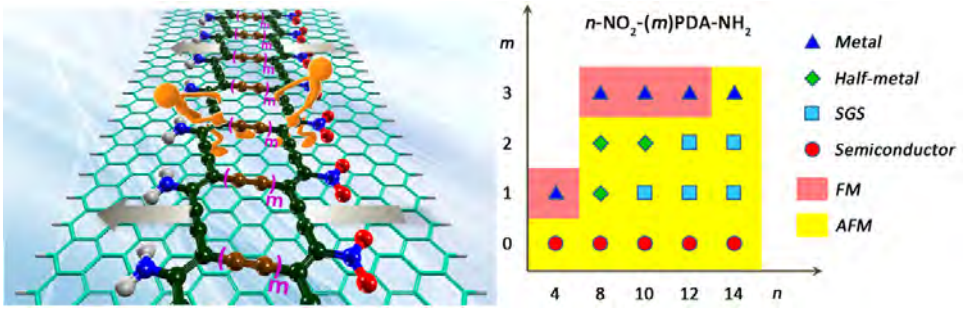

Figure 20. Stacking PDA derivatives on zGNRs via strong π-π interactions can effectively tune the electronic and magnetic properties of zGNRs.

These findings open new opportunities in fabricating new materials for light harvesting, and new electronics and opto-electronics devices, and call for more efforts in using weak interactions for band structure engineering.

1.4. Mechanical properties of graphane, graphene oxide, g-ZnS monolayer and α-moron monolayer

By means of DFT computations, we investigated the mechanical properties of the epoxidized graphene in ordered graphene oxide, namely C_6O_1, C_6O_2, and C_6O_3, representing the carbon : oxygen ratios of 6 : 1, 3 : 1, and 2 : 1, respectively. We predict a reduction of Young's modulus of graphene by a factor of 20%, 23%, and 27% for C_6O_1, C_6O_2, and C_6O_3, respectively, indicating a monotonic degradation with respect to epoxidation. However, there is no clear trend for Poisson's ratio, implying that the local atomic configurations are dominant over oxygen concentrations in determining the Poisson ratio. Our computed high order elastic constants are good for the design of graphene oxide based flexible transparent electronics. These results have been published in *Phys. Chem. Chem. Phys.*, **2015**, 17, 19484.[24]

We investigated the effect of vander Waals interactions on the mechanical properties of hydrogenated single layer homecomb structures, graphane and silicane as two examples, by means of DFT computations. We found that the van der Waals interactions have little effect on the geometry, ultimate strengths, ultimate strains (except biaxial), in-plane stiffness, Poisson ratio, second and third order elastic constants, as expected. However, vdW interactions have significant effect on the fourth and fifth order elastic constants. Such effect is enhanced as the lattice constants or the atom sizes increases. These results have been published in *Mechanics of Advanced Materials and Structures*, **2015**, *22*, 717. [25]

We investigated the mechanical properties and stabilities of g-ZnS monolayers and planar a-boron monolayers under various large strains. The g-ZnS has a low in-plane stiffness, about 1/8 of that of graphene, in comparison, α-Boron has a high in-plane stiffness, about 2/3 of that of graphene, which suggests that α-boron is four times as strong as iron. The higher order elastic constants were also computed. Our

results imply that both g-ZnS and α-boron monolayers are mechanically stable under various large strains. The elastic limits provide a safe-guide for strain-engineering of these 2D materials. These results have been published in *RSC Advances*, **2015**, *5*, 11240,[26] and *Phys. Chem. Chem. Phys.* **2015**, *17*, 2160.[27]

1.5. Computational search for promising LIB electrodes.

Lithium-ion batteries (LIBs) are ubiquitously used in portable and telecommunication electronic devices and are also promising for electric vehicles and electric grid applications. The search for higher specific capacity electrodes is one of the central topics in LIBs, particularly in higher capacity alternatives for graphite anode.

1.5.1. Enhanced Li adsorption and diffusion on MoS_2 and SnS_2 nanoribbons

Layered MoS_2 has ever been proposed as LIB materials. Recently, MoS_2 two-dimensional (2-D) nanosheets and one-dimensional (1-D) nanoribbons with one or few layers have been achieved experimentally, and their performances may be improved as LIB cathode materials. We systematically investigated the adsorption and diffusion of Li atom on MoS_2 bulk, bilayer, monolaye and zigzag MoS_2NRs ($ZMoS_2$NRs) by means of DFT computations. Reducing dimensionality to bilayer and monolayer simultaneously decreases the Li binding energy and diffusion barrier. Due to the edge effect, both the binding strength and the mobility of Li atoms (by lowering the diffusion barrier) can be enhanced in zigzag MoS_2 nanoribbons. Thus, $ZMoS_2$NRs are promising as cathode materials of Li-ion batteries with high power density and fast charge/discharge rate. These results have been published in *J. Phys. Chem. Lett.* **2012**, 3, 2221.[28]

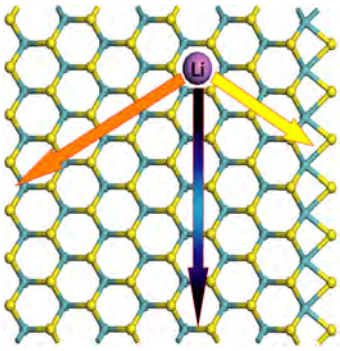

Figure 21. The zigzag MoS_2 nanoribbons as promising lithium-ion battery cathode material (with high Li mobility and strong Li binding energy)

We performed DFT computations to investigate the adsorption and diffusion properties of lithium (Li) on Tin disulfides nanosheets and its derived nanoribbons (NRs), in comparison with SnS_2 bulk in 1T phase. The Li adsorption energies and migration barriers are comparable in SnS_2 bulk and bilayer, and Li adsorbed at the octahedral sites has the highest binding energy in both SnS_2 bulk and bilayer.

Reducing the dimension of SnS_2 to monolayer significantly lowers the Li diffusion barrier while keeping a considerable binding energy, and lithium favors the hollow sites which corresponding to the octahedral sites in bulk phase. Due to the edge effect, SnS_2NRs gain an enhanced Li binding strength, increased Li mobility and improved Li capacity. Thus, SnS_2 nanoribbons are also a promising candidate for anode materials of Li-ion batteries with a high power density and fast charge/discharge rates. These results have been published in *J. Mater. Res.* **2016**, *31*,878.[29]

1.5.2. MoO_3-Based High-Rate LIB Anodes: The Effect of Dimensionality Reduction

By means of DFT computations, we systematically investigated the behavior of lithium (Li) adsorption and diffusion on MoO_3 with different dimensions: including three-dimensional (3D) bulk, two-dimensional (2D) double-layer, 2D monolayer and one-dimensional (1D) nanoribbons. The Li binding energies and diffusion barriers are comparable in MoO_3 bulk and double-layer. Reducing the dimension to the MoO_3 monolayer simultaneously lowers the Li diffusion barrier and the interaction between Li atoms and the MoO_3 monolayer. Cutting the MoO_3 monolayer into 1D nanoribbons can further facilitate the diffusion of Li atoms, and enhance the Li binding energies. Especially, Li diffusion on nanoribbons is rather facile along both the axial and the transverse directions. These computational results demonstrate that due to the dimensional reduction, MoO_3 monolayer nanosheets and nanoribbons have exceptional properties (good electronic conductivity, fast Li diffusion, high operating voltage and high energy density), and thus are promising as high-rate Li ion battery electrodes. These results have been published in *J. Mater. Chem. A.* **2014**, *2*, 19180.[30]

1.5.3. Metallic VS_2 and BSi_3 silicene m*onolayer: promising 2D LIB anode materials*

By means of DFT computations, we systematically investigated the adsorption and diffusion of lithium on the recently synthesized VS_2 monolayer, in comparison with MoS_2 monolayer. Intrinsically metallic, VS_2 monolayer has a higher theoretical capacity (466 mAh/g), a lower Li diffusion barrier than MoS_2, and has a low average open circuit voltage of 0.93 V. Our results suggest that VS_2 monolayer can be utilized as a promising anode material for Li ion batteries with high power density and fast charge/discharge rate. As a new layered inorganic material, VS_2 provides us some basic principles for the enhancement in Li intercalation and diffusion, as well as development guidance for new LIB materials. These results have been published in *J. Phys. Chem. C.* **2013**, *117*, 25409,[31] and was highlighted by www.nanowerk.com.

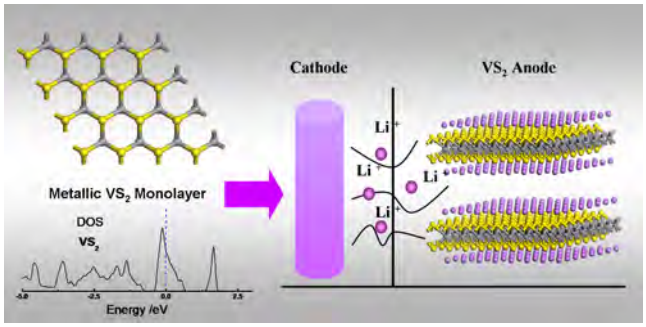

Figure 22. The intrinsically metallic VS_2 monolayers are promising anode materials for LIBs.

Very recently, intrinsically metallic B-substituted silicenes, namely *H*-BSi_3 and *R*-BSi_3 (*H* and *R* denote the hexagonal and rectangular symmetry) have been predicted as the global minimum structures of BSi_3 monolayer (*J. Phys. Chem. C.* **2014**, *118*, 25825). With unusual planar geometry and better electronic conductivity relative to the buckled and semimetallic pristine silicene sheet, the B-substituted silicenes are expected to have good applications in high capacity lithium-ion batteries (LIBs) anode. We systematically investigated the adsorption and diffusion of Li on *H*-BSi_3 and *R*-BSi_3, in comparison with silicene and graphite. Their exceptional properties, including good electronic conductivity, very high theoretical charge capacity (1410 and 846 mA·h/g for single- and double-layer, respectively), fast Li diffusion, and low open circuit voltage (OCV), suggest that the BSi_3 silicene could serve as a promising high capacity and fast charge/discharge rate anode material for LIBs. These results have been published in *J. Phys. Chem. C.* **2014**, *118*, 25836.[32]

1.6. Computational search for promising anchoring materials for lithium-sulfur batteries

In past decades, the lithium-sulfur (Li-S) battery is extensively studied because it plays pivotal roles for the next-generation high-energy rechargeable Li batteries due to its high theoretical capacity and low cost. However, the rapid capacity fading, low Coulombic efficiency, and irreversible loss of active materials have impeded the wide-scale commercial use of Li-S batteries. Trapping the Li_2S_x species to host materials (such as nanomaterials) is an effective way to overcome these challenges.

Phosphorene is a widely studied 2D material recently due to unique puckered structure, outstanding anisotropic physical and mechanism properties, and wide potential applications for the design of nanodevices. By means of DFT computations, we explored the adsorption and diffusion of various Li_2S_x clusters on phosphorene monolayer. Our results revealed that all the Li_2S_x species can moderately bind with phosphorene, exhibit ultrahigh diffusivity along the zigzag direction, and enhance the electrical conductivity of phosphorene. Given these exceptional properties, it is expected that phosphorene can be utilized as a promising anchoring material for high-efficiency Li-S battery cathodes. These results have been published in *J. Mater. Chem. A*, **2016,** 4, 6124.[33]

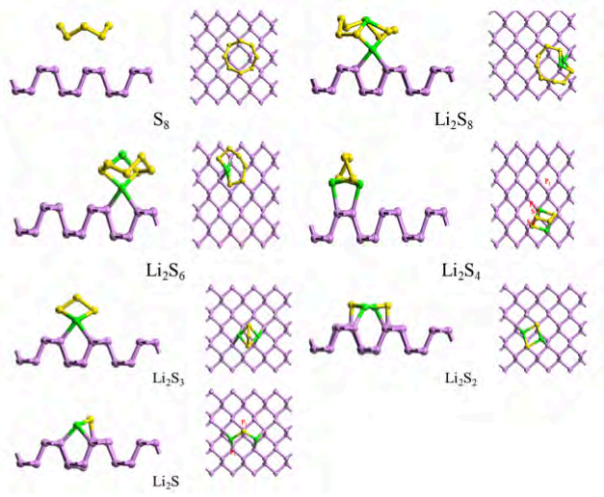

Figure 23. The lowest-energy adsorption configurations of S_8 and Li_2S_x on phosphorene surface,

1.7. Computational search for oxygen reduction reaction (ORR) catalysts

Replacing precious Pt-based catalysts with cheap and earth abundant materials to facilitate the sluggish oxygen reduction reaction (ORR) at the cathode is critical to realize the commercialization of fuel cells. By means of DFT computations, we have identified three promising ORR catalysts based on 2D materials, namely C-doped BN sheets, single-sided fluorine-functionalized graphene, and iron-phthalocyanine (Fe-Pc) monolayer.

Our computations revealed that singly-doping C into *h*-BN nanosheets can cause high spin density and charge density, and reduce the energy gap, resulting in the enhancement of O_2 adsorption. In particular, the C_N sheet (substituting N by C atom) exhibits appropriate chemical reactivity towards O_2 activation, and promotes the subsequent ORR steps to take place though a four-electron OOH hydrogenation pathway with the largest activation barrier of 0.61 eV, which is lower than that of Pt-based catalyst (0.79 eV). Therefore, C_N-based BN sheet is a promising metal-free ORR catalyst for fuel cells in acid media. These results have been published in *J. Phys. Chem. C.* **2015**, *119*, 26348.[34]

We systematically explored the potential of the single-sided chemically functionalized graphene by various functional groups as the metal–free ORR electrocatalyst in alkaline media. Our computations revealed that the spin density due to the single-sided functionalization at 12.5% ratio enhances O_2 adsorption, and the O_2 adsorption energies well correlate with the magnetic moments of C_8R graphenes. C_8F and $C_8(OCH_3)$ graphenes with moderate magnetic moments exhibit appropriate chemical reactivity towards O_2 activation. The following ORR elemental steps prefer to proceed through a $4e^-$ associative pathway, rather than the dissociative and 2e associative pathway. Both C_8F and $C_8(OCH_3)$ graphenes are promising ORR catalysts, and C_8F graphene is more efficient due to its smaller activation barriers and lower overpotential. The present work provides an effective way to tune the catalytic performance of graphene for ORR by introducing a suitable spin density using its

covalent functionalization. These results have been published in *Carbon*, **2016**, 104, 56.[35]

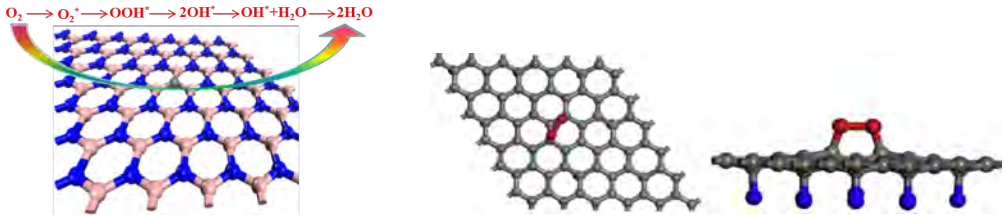

(a) (b)

Figure 24. (a) The C-doped BN nanosheets as ORR catalyst, (b) The top and side views of the lowest-energy configuration of O_2 on C_8F surface.

By means of DFT computations, we demonstrated that the recently synthesized 2D iron-phthalocyanine (Fe-Pc) monolayer, in which the Fe atoms are distributed separately and regularly, is a promising *single-atom-catalyst* for ORR in fuel cells under an acidic environment. Our computations revealed that O_2 molecules can be sufficiently activated on the surface of Fe-Pc monolayer. The subsequent ORR steps on Fe-Pc monolayer prefer to proceed though a more efficient 4e reduction pathway rather than the unfavorable 2e reduction pathway. The theoretical onset potential for ORR on Fe-Pc monolayer can be as high as 0.68 V, which is comparable to that of Pt(111) surface (0.79 V). Especially, Fe-Pc monolayer also has a rather high density of active sites of ~1.5×10^{21} per gram. These advantages make Fe-Pc monolayer a quite promising substitute of Pt catalyst for ORR in fuel cells. Our study is the first theoretical contribution on revealing the possibility of utilizing 2D organometallic sheet as ORR electrocatalyst, and our results do provide a promising candidate for non-Pt ORR catalysts. Actually, besides Fe-Pc monolayer, in recent years more and more 2D organometallic sheets have been synthesized in the laboratory. Our work could provide guidance for rational design and development of novel high-efficient ORR electrocatalysts from various 2D organometallic sheets. These results were just published in *Nanoscale* **2015**, 7, 11633.[36]

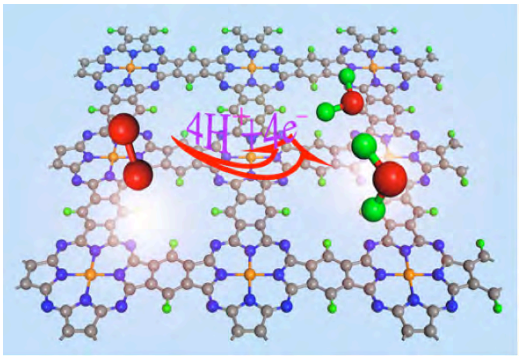

Figure 25. Schematic structure of 2D Fe-Pc monolayer and the key reaction species in ORR.

1.8. Selectivity trend of gas separation through nanoporous graphene

By means of molecular dynamics (MD) simulations, we demonstrate that porous graphene can efficiently separate gases according to their molecular sizes. The flux sequence from the classical MD simulation is $H_2 > CO_2 > N_2 > Ar > CH_4$, which generally follows the trend in the kinetic diameters. This trend is also observed in the computed free energy barriers for gas permeation using the umbrella sampling method. Both classical MD simulations and free energy calcualtions lead to the trend consistent with experiments. The combination of high CO_2 flux and high CO_2/Ar, CO_2/N_2 and CO_2/CH_4 ideal selectivity make nanoporous graphene a promising membrane for CO_2 removal. Case studies of two compositions of CO_2/N_2 mixture further demonstrate the separation capability of nanoporous graphene. These results have been published in *J. Solid State Chem.* **2015**, *224*, 2.[37]

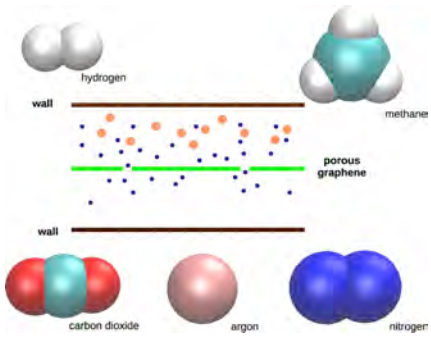

Figure 26. Schematic illustrations of system setup of nanoporous graphene for gas separation along with the gas molecules.

1.9. Preserving the edge magnetism of zigzag graphene nanoribbons by ethylene termination

Edge magnetism is a unique property of graphene ribbons that has been predicted by theory, but not yet directly confirmed experimentally. This could be due to the instability of the ideal zigzag graphene nanoribbons (zGNRs). If researchers want to utilize zGNRs in spintronics, they first need to figure out a suitable termination group for zGNRs. The often used hydrogen atom termination is not a good choice since hydrogen terminated zGNRs can only be stabilized at extremely low hydrogen concentrations. By means of density functional theory computations, we demonstrated that C_2H_4 is the ideal terminal group for zigzag graphene nanoribbons (*z*GNRs) in terms of preserving the edge magnetism with experimental feasibility. The C_2H_4 terminated *z*GNRs (C_2H_4-zGNRs) with pure sp^2 coordinated edges can be stabilized at rather mild experimental conditions, and meanwhile reproduce the electronic and magnetic properties of those hydrogen terminated *z*GNRs. These results have been published in *Scientific Reports*, **2013**, *3*, 2030.[38]

1.10. The effect of hyperconjugation, electronegativities, and conjugation on the electronic and magnetic properties of 2D sandwich nanostructures *(2D) X-Cr-X (X=C_4H, NC_3 and BC_3 monolayer)*

Clar sextet rules have been widely and successfully applied to graphene-related materials, typically the electronic and magnetic properties of such materials can be well rationalized based on this simple rule. For example, the particular stability of partially patterned fluorinated graphene C_4F sheet is due to the so-called "benzation" of graphene (*Phys. Chem. Chem. Phys.* **2013**, *15*, 6842).[39] However, "perturbations" such as conjugation, hyperconjugation may significantly affect the properties, but the importance of such effects has not caught attention so far.

We addressed the importance of the typically overlooked effects, namely hyperconjugation, electronegativities, and conjugation, on the electronic and magnetic properties of two-dimensional (2-D) X-Cr-X (X=C_4H, NC_3 and BC_3 monolayer) sandwich nanostructures. Our systematic computations showed that though featured with the same Clar formulas, these 2-D nanostructures do have different properties. Especially, the very strong π conjugation through the vacant p orbital of the B atom in BC_3 results in its sandwich structure antiferromagic and conducting, which is in stark contrast to the nonmagnetic and semiconducting characters of C_4H-Cr-C_4H and NC_3-Cr-NC_3. Our results suggest that simple counting Clar formulas alone is insufficient to fully understand the electronic and magnetic properties of graphene-related materials, and arouse more attentions to such "perturbation" effects. These results have been published in *Phys. Chem. Chem. Phys.*, **2014**, *16*, 6002.[40]

2. Joint theoretical and experimental studies of 2-D nanomaterials

By joint efforts of theoretical and experimental studies, we have synthesized and characterized MoS_2, MoO_3 and BN monolayers, their derivatives and nanocomposites, developed a convenient chemical approach to modify the morphology of BN nanostructures and a simple approach to etch hexagonal boron nitride monolayers to achieve holes with defined shapes and edges, also observed and carefully analyzed the Moiré Profiles from van der Waals superstructures of boron nitride nanosheets. By DFT computations, we also identified graphene/MoS_2 composites as promsing LIB electrodes, and holey graphenes as ultracapacitor electrodes, which were fabricated and confirmed by our experiments. Moreover, we proposed a new strategy to design and screen organic cathode materials, and confirmed its validity.

2.1. Synthesis and characterization of MoS_2, BN and MoO_3 monolayers

We have synthesized MoS_2 and BN monolayers by liquid exfoliation. Our DFT computations found that the binding energies between MoO_3 monolayer are between those in graphene bilayers and MoS_2 bilayers, which indicates that it is rather feasible to exfoliate MoO_3 monolayer from the bulk using the liquid exfoliation method. Under such a guidance, we also successfully synthesized MoO_3 monolayer and few-layer materials..

2.2. A convenient chemical approach to modify the morphology of BN nanostructures

Our computations showed that energetically it is rather favorable to unzip the BN nanotubes (BNNTs) into BN nanoribbons (Scheme 1).

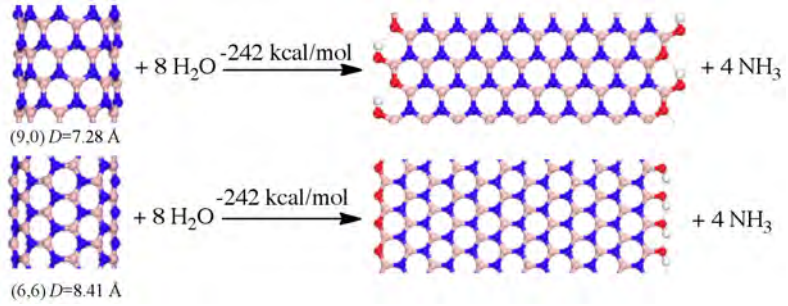

Scheme 1. The computed reaction energy for the hydrolysis process of BN nanotubes

Previous experiment using sonication-assisted hydrolysis to disperse few-layer and monolayer boron nitride nanosheets in water showed that water molecules can attack and dissemble boron-nitride network under continuous sonication. Guided by our computations, we found that, with the presence of ammonia, similar network in boron nitride nanotubes becomes much weakened and more vulnerable to hydrolysis, since as a Lewis base, electron-rich ammonia molecules in a large amount can effectively attach onto the electron-deficient boron atoms on the nanotubes, causing the weakening of the boron-nitride network.

Thus, we developed a very simple process to chemically modify the morphology of BN nanostructures. In this process, the BNNTs can be chemically dispersed and their morphology can be modified by a convenient method - simply sonicating the nanotubes in ammonia water. The dispersed nanotubes are significantly corroded, with end-caps removed, tips sharpened, and walls thinned. The ammonia water-induced corrosion also removes amorphous BN impurities and shorten BNNTs, resembling various oxidative treatments of carbon nanotubes. Importantly, BNNTs were longitudinally unzipped, yielding BN nanoribbons (BNNRs) ~ 5 – 20 nm in widths and up to 1 μm in lengths. Further optimization of the methods led to shortened or unzipped BNNTs. This study may pave the way for convenient processing of the previously-known-inert BNNTs by controlling their dispersion, purity, lengths, and electronic properties. These results have been published in *Adv. Funct. Mater.* **2014**, 24, 4497,[41] and was highlighted by www.nanowerk.com.

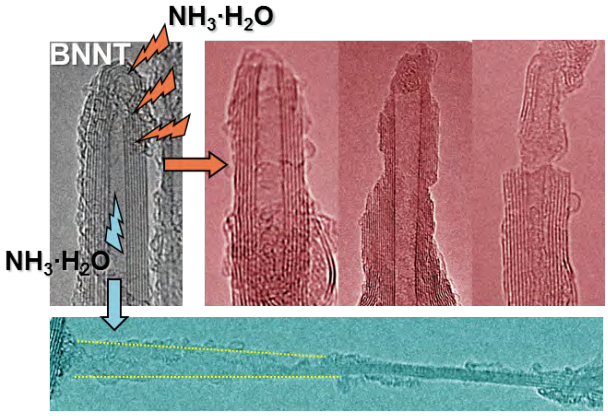

Figure 27. HR-TEM images of the chemically modified BNNTs after hydrolysis

2.3. Oxidative etching of hexagonal boron nitride toward nanosheets with defined edges and holes

Lateral surface etching of 2D nanosheets results in holey 2D nanosheets that have abundant edge atoms. Recent reports on holey graphene showed that holey 2D nanosheets can outperform their intact counterparts in many potential applications such as energy storage, catalysis, sensing, transistors, and molecular transport/separation. From both fundamental and application perspectives, it is desirable to obtain holey 2D nanosheets with defined hole morphology and hole edge structures. This remains a great challenge for graphene and is little explored for other 2D nanomaterials. Here, a facile, controllable, and scalable method is reported to carve geometrically defined pit/hole shapes and edges on hexagonal boron nitride (h-BN) basal plane surfaces via oxidative etching in air using silver nanoparticles as catalysts. The etched h-BN was further purified and exfoliated into nanosheets that inherited the hole/edge structural motifs and, under certain conditions, possess altered optical bandgap properties likely induced by the enriched zigzag edge atoms. This method opens up an exciting approach to further explore the physical and chemical properties of hole- and edge-enriched boron nitride and other 2D nanosheets, paving the way toward applications that can take advantage of their unique structures and performance characteristics. These results have been published *Scientific Reports*, **2015**, *5*, 14510,[42] and were highlighted by SPIE (the international society for optics and photonics) Newsroom.[43]

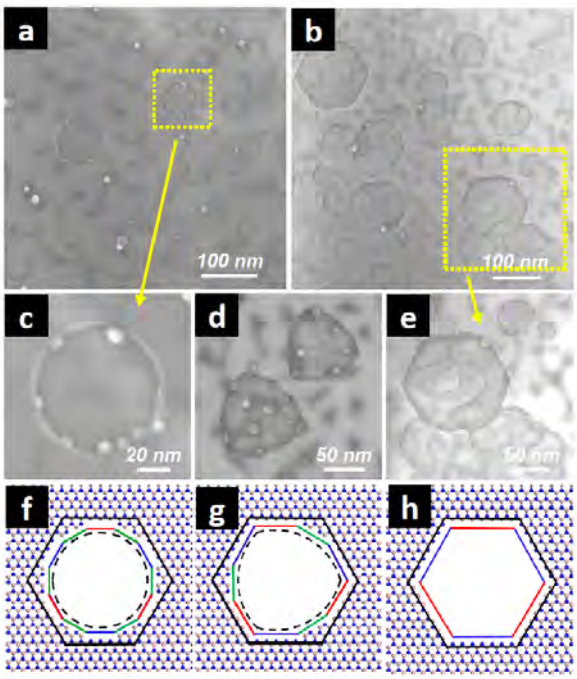

Figure 28. Pit formation on h-BN basal plane due to Ag-catalyzed etching at 800 °C for 3 h. (**a**) and (**b**) are SEM images of the h-BN basal plane surface at lower magnifications where multiple circular and hexagonal pits formed, respectively. (**c**) – (**e**) are close-up SEM images of pits with shapes of a circle, Reuleaux triangles, and a hexagon, respectively. (**f**) – (**h**) are the corresponding atomic models for (c) – (e).

2.4. Evolution of Moiré profiles from van der Waals superstructures of BN nanosheets

Two-dimensional (2D) van der Waals (vdW) superstructures, or vdW solids, are formed by the precise restacking of 2D nanosheet lattices, which can lead to unique physical and electronic properties that are not available in the parent nanosheets. Moiré patterns formed by the crystalline mismatch between adjacent nanosheets are the most direct features for vdW superstructures under microscopic imaging.

We reported the transmission electron microscopy (TEM) observation of hexagonal Moiré patterns with unusually large micrometer-sized lateral areas (up to ~1 μm^2) and periodicities (up to ~50 nm) from restacking of liquid exfoliated hexagonal boron nitride nanosheets (BNNSs). This observation was attributed to the long range crystallinity and the contaminant-free surfaces of these chemically inert nanosheets. Parallel-line-like Moiré fringes with similarly large periodicities were also observed. The simulations and experiments unambiguously revealed that the hexagonal patterns and the parallel fringes originated from the same rotationally mismatched vdW stacking of BNNSs and can be inter-converted by simply tilting the TEM specimen following designated directions. This finding may pave the way for further structural decoding of other 2D vdW superstructure systems with more complex Moiré images. These results have been published in *Scientific Reports*, **2016**, *6*, 26084.[44]

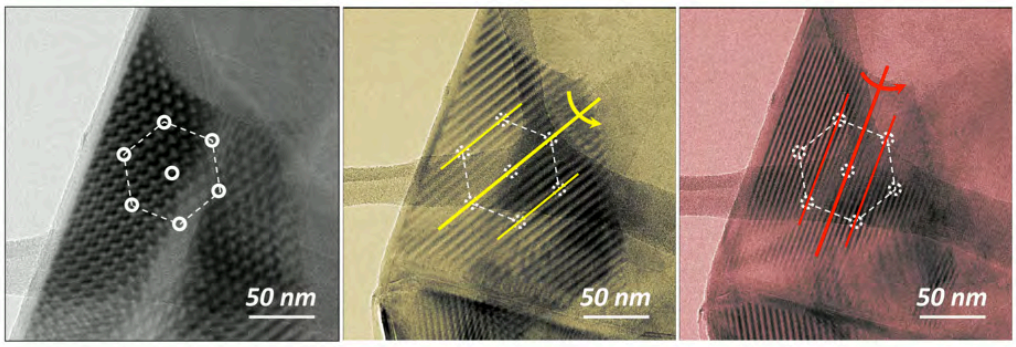

Figure 29. Moiré profiles from van der Waals superstructures of BN nanosheets

2.5. Layer-by-layer hybrids of MoS_2 and reduced graphene oxide (rGO) for lithium ion batteries

Two-dimensional MoS_2 shows high potential for effective Li storage due to its high thermal and chemical stability, high theoretical capacity, and experimental accessibility. However, the poor electrical conductivity and the restacking tendency significantly restrict its applications to lithium ion batteries (LIBs). To overcome these problems, we introduce reduced graphene oxides (rGO) to the intercalation-exfoliation preparation process of few-layered MoS_2 and obtain layer-by-layer MoS_2/rGO hybrids. With the addition of rGO, the restacking of MoS_2 layers is well inhibited, and MoS_2 with 1~3 layers is obtained in the composites. Due to the positive role of rGO, MoS_2/rGO hybrids exhibit highly enhanced cyclic stability and high-rate performances as LIB anodes in comparison with bare MoS_2 layers or bulk MoS_2. Moreover, the experimental results are well interpreted through density functional theory computations. These results have been published in *Electrochimica Acta*, **2014**, *147*, 392.[45]

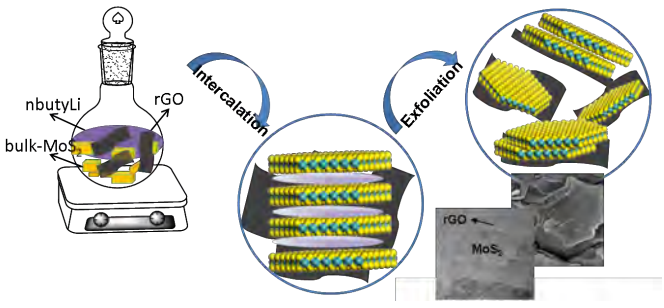

Figure 30. The process of synthesize the layer-by-layer hybrids of MoS_2 and rGO.

2.6. Scalable holey graphene synthesis and dense electrode fabrication toward high performance ultracapacitors

By joint theoretical and experimental efforts, we developed a scalable synthesis method of holey graphene (h-Graphene) in a single step without using any catalysts or special chemicals. The film made of the as-synthesized h-Graphene exhibited relatively strong mechanical strength, 2D hole morphology, high density, and facile processability. This scalable one-step synthesis method for h-Graphene is time-efficient, cost-efficient, environmentally friendly, and generally applicable to other two-dimensional materials. The ultracapacitor electrodes based on the h-Graphene show a remarkably improved volumetric capacitance with about 700% increase compared to that of regular graphene electrodes. These results have been published in *ACS Nano*, **2014**, *8*, 8255.[46]

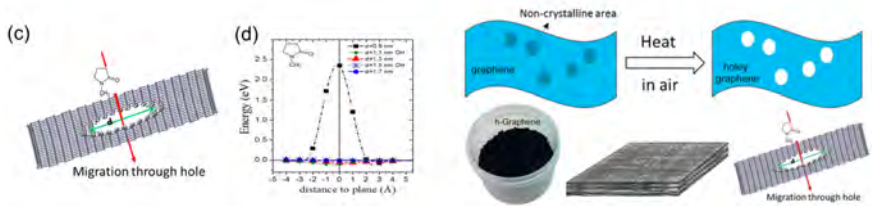

Figure 31. (Left) The relative energies with respect to the molecule at a large distance from the h-Graphene plan for the EMI^+ rigidly migrating through the hole, (right) the experimental scheme to fabricate holey graphene for ultracapacitors

2.7. Designing high-voltage carbonyl-containing polycyclic aromatic hydrocarbon cathode materials for Li-ion batteries guided by Clar's theory

Developing future batteries requires low-cost electrode materials with high energy and power density. Among numerous emerging battery technologies, organic electrode batteries, which only contain light and earth-rich elements, are rather promising. Several carbonyl-containing polycyclic aromatic hydrocarbons (C-cPAHs) have shown excellent performance as cathode materials for Li-ion batteries (LIBs). However, their low voltages seriously hinder the development of organic batteries with high energy density, and currently most theoretical and experimental efforts are based on trial and error strategy.

By means of DFT computations, we examined the correlation between the electron delocalization (aromaticity) and the lithiation voltage of carbonyl-containing polycyclic aromatic hydrocarbonss. Our analyses revealed that the correlation can be well explained by the Clar's aromatic sextet theory. An index denoted as ΔC_{2Li} is introduced to characterize aromaticity change during lithiation. Several molecules with high ΔC_{2Li} and high voltage were designed, and we also experimentally investigated a molecule with positive ΔC_{2Li}, namely 1,4,5,8-phenanthrenediquinone

(PADQ), as the cathode material. Our proposed design strategy provides an efficient and effective way to design and screen carbonyl-containing PAH-based cathode materials. More promising organic electrode materials can be discovered by our strategy, including some experimentally available organic molecules whose promise as electrodes has not been explored. These results have been reported in *J. Mater. Chem. A.* **2015**, *3*, 19137.[47]

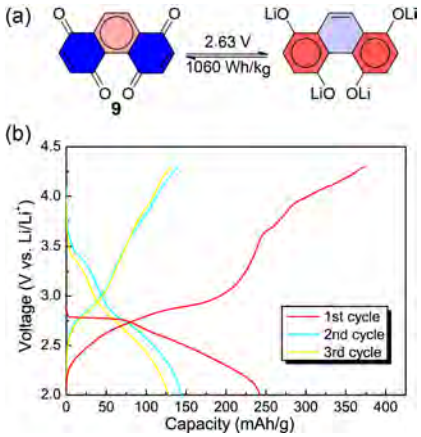

Figure 32. Molecular structure of PADQ, the lithiation reaction, the calculated voltage and energy density. (b) Charge-discharge curves of the first three cycles

3. Book and review article about 2-D nanomaterials

I co-edited a book,[48] "Graphene Chemistry: Theoretical Perspectives", with Dr. De-en Jiang (Oak Ridge National Lab), which was published by John Wiley & Sons in 2013. In this book, we contributed five chapters, in which we discussed the general aspect of theoretical graphene chemistry,[49] how to understand the aromaticity of graphene and graphene nanoribbons by Clar sextet rule,[50] overviewed the most recent progress for he conversion between graphene and graphene oxide,[51] and application of graphene-related materials in catalysis [52] and hydrogen storage.[53]

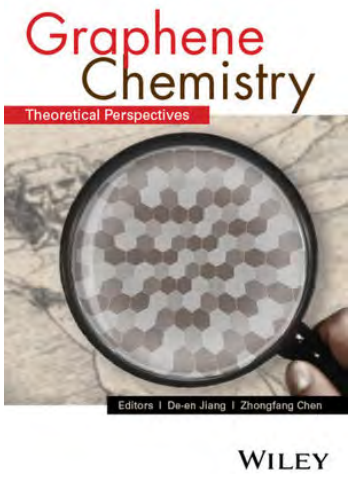

We published a comprehensive review on graphene chemistry titled "Graphene-related Nanomaterials: Tuning Properties by Functionalization" (*Nanoscale*, **2013**, 5, 4541).[54]

We also contributed a comprehensive review summarizing the on-going efforts and studies from both experimental and theoretical communities on developing graphene, inorganic graphene analogues (IGAs) and their composites as LIB electrodes. Compared with graphene, we put more emphasis on IGAs, such as transition metal oxides, dichalcogenides, and MXene, and illustrated the great advantages of IGAs as electrodes. We also showed that due to the effective synergic interactions between graphene and IGAs, their composites step further to achieve reversible high-capacity LIBs. Finally, we also discussed the problems and barriers for the practical applications of 2D materials to LIBs. Besides presenting the most recent developments in this field to our peers, this review also serves as a guideline for our further studies in developing IGA-based LIB electrodes. This review was published in *J. Mater. Chem. A.* **2014**, *2*, 12104.[55]

Upon the invitation by WIREs *Computational Molecular Science*, we presented a advanced review to summarize our recent efforts computational investigations of graphene-like materials, mostly funded by this DoD grant. DFT computations offer a powerful tool to investigate the electronic structure (principally the ground state) of nanomaterials, to predict their intrinsic properties, assist in characterization and rationalization of experimental findings, as well as explore their potential applications. By DFT computations, many graphene-like materials have been explored and designed, and fantastic properties are disclosed. In this overview, we present the recent computational progress in discovering the intrinsic structural, electronic and magnetic properties of several important and representative graphene-like 2D nanomaterials, as well as identifying their potential applications. The highlighted graphene-like structures include layered van der Waals (vdW) materials (*h*-BN, MoS_2, α-MoO_3, and V_2O_5), graphitic-like ZnO, MXenes (metal carbides or carbonitrides), the not-yet-synthesized B_2C, SiC_2, BSi_3, arsenene and antimonene, and single-layer coordination polymers ($[Cu_2Br(IN)_2]_n$ (IN = isonicotinato), Fe-phthalocyanine, and nickel bis(dithiolene)). This review has been published in *WIREs Computational Molecular Science*, **2015**, *5*, 360.[56]

Upon the invitation by *Angew Chem*, we presented a comprehensive review to summarize the emergence and growth of the field of planar hypercoordinate chemistry over more than four decades. We delineated the evolution of such planar configurations from small molecules to clusters, to nanospecies and to bulk solids. Some experimentally fabricated planar materials have been shown to possess unusual electrical and magnetic properties. A fundamental understanding of planar hypercoordinate chemistry and its potential will help guide its future development. This review has been published in *Angew. Chem. Int. Ed.* **2015**, 54, 9468.[57]

4. Other research work

By means of the most sophisticated dissected CMO (canonical molecular orbital)-NICS (nucleus independent chemical shifts) analysis and energetic

evaluations, we found that C_{60} does not have "superaromatic" or even aromatic character, but is a highly strained and spherically π antiaromatic species! (*Phys. Chem. Chem. Phys.* **2012**, *4*, 14886).[58] We identified new members of C_{70} homofullerenes inspired by the Bent's rule (*J. Theor. Comput. Chem.* **2013**, *12*, 1250097),[59] and a fullerene-like $C_{12}B_{68}$ cluster containing multiple quasi-planar tetracoordinated carbon moieties (*J. Mol. Mod.* **2014**, *20*, 2085). [60] We identified two magnetic matryoshka superatoms, i.e., $Sn@Mn_{12}@Sn_{20}$ and $Pb@Mn_{12}@Pb_{20}$, which possess large magnetic moment of 28 μ_B and moderate HOMO-LUMO gaps (*Scientific Reports* **2014**, *4*, 6915).[61]

We investigated the dynamic motion of an encapsulated Lu pair inside a $C_{76}(T_d)$ cage (*RSC Advance*, **2015**, *5*, 34383),[62] and the structures, stabilities and electronic properties of the endohedral derivatives $M@B_{40}$ (M = Sc, Y, La) (*Theor. Chem. Acc.* **2015**, *134*, 13).[63] We also contributed two comprehensive reviews on metal carbide clusterfullerenes (*Coord. Chem. Rev.* **2014**, *270-271*, 89)[64] and magnetic clusters (*Coord. Chem. Rev.* **2015**, *289-290*, 315).[65]

We designed many molecules with novel chemical bonding, such as $M©B_n$ boron wheels containing planar hypercoordinated central atom M (*Phys. Chem. Chem. Phys.* **2012**, *14*, 14898).[66] We carefully evaluated the performance of the density functional methods in describing the intermolecular interactions in the methane hydrates and recommended appropriate approaches to study the noncovalent interactions in such systems.[67]

We explored the origin of the enhanced photocatalytic activity of the Mo-doped monoclinic $BiVO_4$ (*Phys. Chem. Chem. Phys.* **2014**, *16*, 3465),[68] and provided deeper understanding of different photocatalytic activities of $BiMO_4$ (M=V, Nb, Ta) (*J. Mater. Chem. A*, **2014**, *2*, 8294).[69]

We continued our fruitful collaborations with experimentalists. We assisted the structural characterization of the endohedral clusterfullerene (EMF) entrapping an yttrium cyanide cluster inside a popular C_{82} cage—$YCN@C_s(6)\text{-}C_{82}$ (*Scientific Reports* **2013**, *3*, 1487), [70] and some new porphyrin or metalloporphyrin macrocycle-containing model complexes to mimic the active site of [FeFe]-hydrogenases (*J. Mater. Chem. A*, **2014**, *2*, 8294).[71]

5. Some highlights

(1) Our paper titled "Oxidative Etching of Hexagonal Boron Nitride Toward Nanosheets with Defined Edges and Holes" (*Scientific Reports*, **2015**, *5*, 14510) was highlighted

by SPIE (the international society for optics and photonics) Newsroom (SPIE Newsroom. **201**6, DOI: 10.1117/2.1201512.006248)

(2) Eleven (11) papers were highlighted as cover pictures of scientific journals.

J. Comput. Chem.
2013, *34*,121

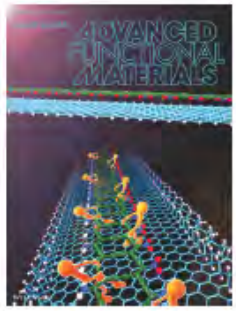

Adv. Funct. Mater.
2013, *22*, 1507

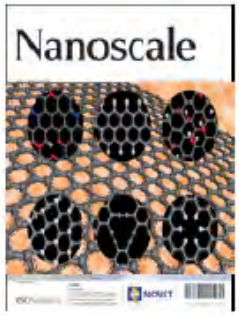

Nanoscale
2013, 5, 4541

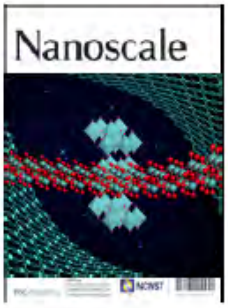

Nanoscale
2013, 5, 5321

J. Chem. Theor. Comput.
2014, 10, 1265

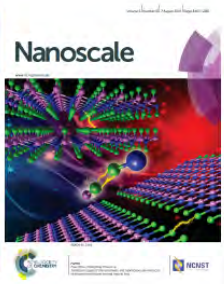

Nanoscale
2014, 6,8624

Angew. Chem. Int. Ed
2014, 53, 7248

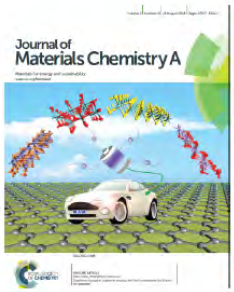

J. Mater. Chem. A
2014, 2, 12077

Adv. Funct. Mater.
2014, *24*, 4497

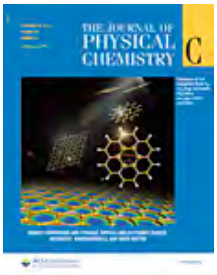

J. Phys. Chem. C
2014, *118*,25836

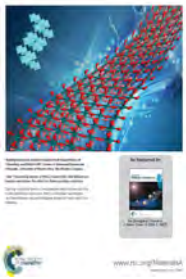

J. Mater. Chem. A
2014, *2*, 19180

(3) Eight (8) papers were highlighted by www.nanowerk.com, a leading website committed to educate, inform and inspire about nanosciences, nanotechnologies and other emerging technologies.

- Li, Y. Li, F.; Chen, Z. Graphane/Fluorographene Bilayer: Considerable C–H···F–C Hydrogen Bonding and Effective Band Structure Engineering, *J. Am. Chem. Soc.* **2012**, *134*,11269–11275.

- Li, Y.; Chen, Z. XH/π (X = C, Si) Intractions in Graphene and Silicene: Weak in Strength, Strong in Tuning Band Structures, *J. Phys. Chem. Lett.* **2013**, *4*, 269-275.

- Li, Y.; Zhou, Z.; Cabrera, C. R.; Chen, Z. Preserving the Edge Magnetism of Zigzag Graphene Nanoribbons by Ethylene Termination: Insight by Clar's Rule, *Scientific Reports*, **2013**, *3*, 2030.

- *Liao, Y.; Chen, Z. Connell, J. W.; Fay, C. C.; Park, C.; Kim, J. W. ; Li, Y.* Chemical Sharpening, Shortening, and Unzipping of Boron Nitride Nanotubes, *Adv. Funct. Mater.* **2014**, *24*, 4497-4506.

- Jing, Y.; Zhou, Z.; Cabrera, C. R.; Chen, Z. Metallic VS_2 Monolayer: A Promising 2D Anode Material for Lithium Ion Batteries, *J. Phys. Chem. C.* **2013**, *117*, 25409–25413.

- Liao, Y.; Tu, K.; Han, X.; Hu, L.; Connell, J.; Chen, Z.; Lin, Y. Oxidative Etching of Hexagonal Boron Nitride Toward Nanosheets with Defined Edges and Holes, *Scientific Reports*, **2015**, *5*, 14510.

- Zhang, S.; Yan, Z.; Li, Y.; Chen, Z.; Zeng, H. Atomically Thin Arsenene and Antimonene: Semimetal-Semiconductor and Indirect-Direct Band Gap Transitions, *Angew. Chem. Int. Ed.* **2015**, *54*, 3112-3115.

- Zhao, J.; Yang, Y.; Katiyar, R. S.; Chen, Z. Phosphorene as a Promising Anchoring Material for Lithium-Sulfur Batteries: A Computational Study, *J. Mater. Chem. A*, **2016,** 4, 6124-6130

(3) Our paper on theoretical prediction of arsenene and antimonene (*Angew. Chem. Int. Ed.* **2015**, *54*, 3112-3115) was highlighted by the following media

Nature 2015, 517, 246:
http://www.nature.com/nature/journal/v517/n7534/pdf/517246c.pdf

RESEARCH HIGHLIGHTS

Gut microbes' survival tactics

Monkey in the mirror

Arsenic forms a semiconductor

Lungs began with many chambers

Resource use peaks worldwide

ChemistryViews:
http://www.chemistryviews.org/details/ezine/7241602/As_and_Sb_Monolayers_as_2D_Semiconductors.html

MaterialsViews:
http://www.materialsviewschina.com/2015/01/15239/

(4) We have been actively participated outreach activities.

- Chemistry Magic Show, Oct. 17, 2012, Central School of Visual Arts, Santruce, Team members Jessica M. Gonzalez Delgado and two other undergraduate students.
- Chemistry Magic Show, May 17, 2013, St. John's School, San Juan, Puerto Rico.
- Computational chemistry demostration for NanoDays, Apr. 12-13, 2013, San Juan, Puerto Rico.
- "Chinese Culture" (emphasizing Chinese Spring Festival), Dec. 6, 2012, St. John's School, San Juan, Puerto Rico
- Participating Chemistry Festival in Old San Juan, Oct. 21, 2012. Experimental demonstration "Color Challenging Milk" to explain "How Soap Works"; Nanotoxicity Awareness Survey. The team including my graduate and undergraduate students, and four children: Jerry Chen (6 years old), Karen Gao (11), Samel Samehyahya (10), Chunxiao Gao (13).

How we do the Nanotoxicity survey: (1) two girls played violin to attract the audience; (2) together with other team members, they gave the people with interest short introductions about nanomaterials and their potential negative effects; (3) the people voted about if they were willing to buy the tomato with nano-fertilizers.

- Participating Chemistry Festival in Old San Juan, April 27, 2014. Experimental demonstration "Color Challenging Milk" to explain "How Soap Works"; Nanotoxicity Awareness Survey. The team including my graduate and undergraduate students, and seven children: Jerry Chen (7 years old), Kit Jackson

(7), Karen Gao (12), Katherine Tsui (12), Juliana Feng (12), Serena Tsui (14), Michaelle Gao (15).

- "Chinese Culture" (emphasizing Chinese Spring Festival), Feb. 7, 2014, St. John's School, San Juan, Puerto Rico
- Participating Chemistry Festival in Old San Juan, October 26, 2014. Experimental demonstration "Color Challenging Milk" to explain "How Soap Works"; Nanotoxicity Awareness Survey. The team including my graduate and undergraduate students, and six children: Jerry Chen (8years old), Karen Gao (12), Katherine Tsui (13), Juliana Feng (13), Serena Tsui (15), Michaelle Gao (15).

(5) Noticeable achievements of our students

- Two graduate students, Fengyu Li (female) and Yunlong Liao, got the prestigious, merit-based fellowship from Institute for Functional Nanomaterials, University of Puerto Rico.
- Our undergraduate student researcher, Ms. Jessica M. Gonzalez Delgado (female), got RISE fellowship to support her undergraduate research, and entered North Carolina State University, to continue graduate studies.
- Our undergraduate student researcher, Cristian Morales, University of Puerto Rico, entered University of Pittsburgh for graduate studies, and just won the NSF Fellowship.
- Our high school student researcher, Jiacheng Feng, published a first author paper, and was admitted to MIT. He continued to demonstrate his excellence there, got two BS degree (mathematics and economy), and was just admitted to Harvard for graduate studies.
- At the age of 14, our high school student researcher, Michell Gao, gave an scientific talk, "*Tomato as messengers of Nanotoxicity awareness in Society*", in the 48th ACS Junior Technical Meeting / 33rd Puerto Rico Interdisciplinary Scientific Meeting (PRISM) on March 9, 2013
- Michelle Gao (female) was admitted to both MIT and Duke, and will go to Duke for college in this August.
- Our high school student researcher, Esmarline De Leon Peralta (female), entered UPR Mayaguez for college.
- Fengyu Li (female) got PhD in 2014, and Yunlong will defend PhD dissertation at the end of this May. Fuzhao Li has finished his MS research, and will defend his dissertation in the summer.

References

[1] Li, Y.; Liao, Y.; Schleyer, P. v.R.; Chen, Z. Al_2C Monolayer: The Planar Tetracoordinate Carbon Global Minimum, *Nanoscale*, **2014,** 6, 10784.

[2] Li, Y.; Liao, Y.; Chen, Z. Be_2C Monolayer with Quasi-Planar Hexacoordinate Carbons: A Global Minimum Structure, *Angew. Chem. Int. Ed*. **2014**, *53*, 7248 –7252.

[3] Wang, Y.; Li, F.; Li, Y.; Chen, Z. Semimetallic Be_5C_2 Monolayer Global Minimum with Quasi-Planar Pentacoordinate Carbons and Negative Possion's Ratio, *Nature Communications*, **2016**, *7*, 11488.

[4] Zhang, H.; Li, Y.; Hou, J.; Tu, K.; Chen, Z. FeB_6 Monolayers: The Graphene-like Material with Hypercoordinate Transition Metal, *J. Am. Chem. Soc.* **2016**, *138*, 5644–5651.

[5] Zhang, S.; Yan, Z.; Li, Y.; Chen, Z.; Zeng, H. Atomically Thin Arsenene and Antimonene: Semimetal-Semiconductor and Indirect-Direct Band Gap Transitions, *Angew. Chem. Int. Ed.* **2015**, *54*, 3112-3115.

[6] Zhang, S.; Xie, M.; Li, F.; Yan, Z.; Li, Y.; Kan, E.; Liu, W.; Chen, Z.; Zeng, H. Semiconducting Group 15 Monolayers: A Broad Range of Band Gaps and High Carrier Mobilities, *Angew. Chem. Int. Ed.* **2016**, *55*, 1666-1669.

[7] Ma, F.; Zhou, M; Jiao, Y.; Gao, G.; Gu, Y.; Bilic, A.; Chen, Z.; Du, A. Single Layer Bismuth Iodide: Computational Exploration of Structural, Electrical, Mechanical and Optical Properties, *Scientific Reports*, **2015**, *5*, 17558.

[8] Wang, Y.; Li, Y.; Chen, Z. Not Your Familiar Two Dimensional Transition Metal Disulfide: Structural and Electronic Properties of PdS_2 Monolayer, *J. Mater. Chem. C.* **2015**, *3*, 9603 – 9608.

[9] Li, F.; Tu, K; Zhang, H.; Chen, Z. Flexible Structural and Electronic Properties of Pentagonal B_2C Monolayer via External Strain: A Computational Investigation, *Phys. Chem. Chem. Phys*. **2015**, 17, 24151-24156.

[10] Tan, X.; Li, F.; Chen, Z. Metallic BSi_3 Silicene and Its One-Dimensional Derivatives: Unusual Nanomaterials with Planar Aromatic D_{6h} Six-Membered Silicon Rings, *J. Phys. Chem. C*. **2014**, *118*, 25825-25835.

[11] Li, F.; Tu, K.; Chen, Z. Versatile Electronic Properties of VSe_2 Bulk, Few-Layers, Monolayer, Nanoribbons, and Nanotubes: A Computational Exploration, *J. Phys. Chem. C.* **2014**, *118*, 21264–21274.

[12] Liu, Q.; Li, L.; Li, Y.; Gao, Z.; Chen, Z. Lu, J. Tuning Electronic Structure of Bilayer MoS_2 by Vertical Electric Field: A First-Principles Investigation, *J. Phys. Chem. C.* **2012**, *116*, 21556–21562.

[13] Li, Y.; Chen, Z. Tuning Electronic Properties of Germanane Layers by External Electric Field and Biaxial Tensile Strain: A Computational Study, *J. Phys. Chem. C*, **2014**, *118*, 1148-1154.

[14] Li, F.; Chen, Z. Tuning Electronic and Magnetic Properties of MoO_3 Sheets by Cutting, Hydrogenation, and External Strain: A Computational Investigation, *Nanoscale*, **2013**, 5, 5321-5333.

[15] Zhang, H.; Ma, Y.; Chen, Z. Quantum Spin Hall Insulators in Strain-modified Arsenene, *Nanoscale*, **2015**, *7*, 19152-19159.

[16] Liao, Y.; Chen, Z. Uniform Bending Effect on Electronic Properties of Boron

Nitride Nanoribbons: A Computational Investigation, *Nano Life*, **2012**, 2, 1240005.

[17] Wang, Y.; Li, Y.; Chen, Z. Reducing Band Gap and Enhancing Carrier Mobility of Boron Nitride Nanoribbons by Conjugated ∏ Edge States, *J. Phys. Chem. C.* **2014**, *118*, 25051–25056.

[18] Li, Y.; Li, F.; Chen, Z. Graphane/Fluorographene Bilayer: Considerable C−H···F−C Hydrogen Bonding and Effective Band Structure Engineering, *J. Am. Chem. Soc.* **2012**, *134*,11269–11275.

[19] Li, Y.; Pantoja, B. A.; Chen, Z. Self-modulated Band Structure Engineering in C_4F Nanosheets: First-Principles Insights, *J. Chem. Theory Comput.* **2014,** *10*, 1265-1271.

[20] Li, Y.; Chen, Z. XH/π (X = C, Si) Intractions in Graphene and Silicene: Weak in Strength, Strong in Tuning Band Structures, *J. Phys. Chem. Lett*. **2013**, *4*, 269-275.

[21] Tang, Q.; Zhou, Z.; Shen, P.; Chen, Z. Band Gap Engineering of BN sheet by Interlayer Dihydrogen Bonding and Electric Field Control, *ChemPhysChem* **2013**, *14*, 1787-1792.

[22] Tang, Q.; Bao, J.; Li, Y.; Zhou, Z.; Chen, Z. Tuning Band Gaps of BN Nanosheets and Nanoribbons via Interfacial Dihalogen Bonding and External Electric Field, *Nanoscale* **2014**, *6*, 8624-8634.

[23] Guan, J.; Chen, W.; Li, Y.; Yu, G.; Shi, Z.; Huang, X.; Sun, C.; Chen, Z. An Effective Approach to Achieve Spin Gapless Semiconductor – Half-Metal – Metal Transition in Zigzag Graphene Nanoribbons: Attaching A Floating Induced Dipole Field via π-π Interactions, *Adv. Funct. Mater.* **2013**, *23*, 1507-1518.

[24] Peng, Q.; Han, L.; Lian, J.; Wen, X.; Liu, S.; Chen, Z.; Koratkar, N.; De, S. Mechanical Degradation of Graphene by Epoxidation: Insight from First-principles Calculations, *Phys. Chem. Chem. Phys.*, **2015**, 17, 19484-19490.

[25] Peng, Q.; Chen, Z.; De, S. A Density Functional Theory Study of the Mechanical Properties of Graphane with van der Waals Corrections, *Mechanics of Advanced Materials and Structures*, **2015**, *22*, 717.

[26] Han, L.; Peng, Q.; Huang, C.; Wen, X.; Liu, S.; Chen, Z.; Lian, J.; De, S. Mechanical properties and stabilities of g-ZnS monolayers, *RSC Advances*, **2015**, *5*, 11240 – 11247.

[27] Peng, Q.; Han, L.; Wen, X.; Liu, S.; Chen, Z.; Lian, J.; De, S. Mechanical Properties and Stabilities of α-Boron Monolayers, *Phys. Chem. Chem. Phys.* **2015**, *17*, 2160-2168.

[28] Li, Y.; Wu, D.; Zhou, Z.; Cabrera, C.; Chen, Z. Enhanced Li Adsorption and Diffusion on MoS_2 Zigzag Nanoribbons by Edge Effects - A Computational Study, *J. Phys. Chem. Lett.* **2012**, 3, 2221–2227.

[29] Tu, K.; Li, F.; Chen, Z. Enhanced Lithium Adsorption/Diffusion and Improved Li Capacity on SnS_2 Nanoribbons: A Computational Investigation, *J. Mater. Res.* **2016**, *31*,878-885.

[30] Li, F.; Cabrera, C. R.; Chen, Z. Theoretical Design of MoO_3-Based High-Rate Lithium Ion Battery Electrodes: The Effect of Dimensionality Reduction, *J. Mater. Chem. A.* **2014**, *2*, 19180-19188.

[31] Jing, Y.; Zhou, Z.; Cabrera, C. R.; Chen, Z. Metallic VS_2 Monolayer: A Promising 2D Anode Material for Lithium Ion Batteries, *J. Phys. Chem. C.* **2013**, *117*, 25409–25413.

[32] Tan, X.; Chen, Z. Metallic BSi_3 Silicene: A Promising High Capacity Anode Material for Lithium-Ion Batteries, *J. Phys. Chem. C*. **2014**, *118*, 25836–25843

[33] Zhao, J.; Yang, Y.; Katiyar, R. S.; Chen, Z. Phosphorene as a Promising Anchoring Material for Lithium-Sulfur Batteries: A Computational Study, *J. Mater. Chem. A*, **2016,** 4, 6124-6130.

[34] Zhao, J.; Chen, Z. Carbon-doped BN Nanosheet: An Efficient Metal-Free Electrocatalyst for the Oxygen Reduction Reaction, *J. Phys. Chem. C.* **2015** , *119*, 26348–26354.

[35] Zhao, J.; Cabrera, C. R.; Xia, Z.; Chen, Z. Single–sided Fluorine–functionalized Graphene: a Metal–free Electrocatalyst with High Efficiency for Oxygen Reduction Reaction, *Carbon*, **2016**, *104*, 56-63.

[36] Wang, Y.; Li, Y.; Chen, Z. Two-Dimensional Iron-Phthalocyanine (Fe-Pc) Monolayer As a Promising Single-Atom-Catalyst for Oxygen Reduction Reaction: A Computational Study, *Nanoscale*, **2015**, *7*, 11633-11641.

[37] Liu, H.; Chen, Z.; Dai, S.; Jiang, D. E. Selectivity Trend of Gas Separation through Nanoporous Graphene, *J. Solid State Chem.* **2015**, *224*, 2-6.

[38] Li, Y.; Zhou, Z.; Cabrera, C. R.; Chen, Z. Preserving the Edge Magnetism of Zigzag Graphene Nanoribbons by Ethylene Termination: Insight by Clar's Rule, *Scientific Reports*, **2013**, *3*, 2030.

[39] Popov, I. A.; Li, Y.; Chen, Z.; Boldyrev, A. I. "Benzation" of graphene upon addition of monovalent chemical species, *Phys. Chem. Chem. Phys.* **2013**, *15*, 6842-6848

[40] Tan, X.; Jin, P.; Chen, Z. With the Same Clar Formulas, Do the Two-dimensional Sandwich Nanostructures X-Cr-X (X=C_4H, NC_3 and BC_3) Behave Similarly? *Phys. Chem. Chem. Phys.*, **2014**, *16*, 6002-6011.

[41] Liao, Y.; Chen, Z.; Connell, J. W.; Fay, C. C.; Park, C.; Kim, J. W.; Lin, Y. Chemical Sharpening, Shortening, and Unzipping of Boron Nitride Nanotubes, *Adv. Funct. Mater*. **2014**, *24*, 4497-4506.

[42] Liao, Y.; Tu, K.; Han, X.; Hu, L.; Connell, J.; Chen, Z.; Lin, Y. Oxidative Etching of Hexagonal Boron Nitride Toward Nanosheets with Defined Edges and Holes, *Scientific Reports*, **2015**, *5*, 14510.

[43] Liao, Y.; Chen, Z.; Connell, J. W.; Lin, Y. Putting the holes in holey white graphene, SPIE Newsroom. **201**6, DOI: 10.1117/2.1201512.006248

[44] Liao, Y.; Cao, W.; Connell, J. W.; Chen, Z.; Lin, Y. Evolution of Moiré Profiles from van der Waals Superstructures of Boron Nitride Nanosheets, *Scientific Reports*, **2016**, *6*, 26084.

[45] Jing, Y.; Ortiz-Quiles, E. O.; Cabrera, C. R.; Chen, Z.; Zhou, Z. Layer-by-Layer Hybrids of MoS_2 and Reduced Graphene Oxide for Lithium Ion Batteries, *Electrochimica Acta*, **2014**, *147*, 392–400.

[46] Han, X.; Funk, M. R.; Shen, F.; Chen, Y. C.; Li, Y.; Campbell, C. J.; Dai, J.; Kim,

J. W.; Liao, L.; Connell, J. W; Barone, V.; Chen, Z.; Lin, Y.; Hu, L. Scalable Holey Graphene Synthesis and Dense Electrode Fabrication Toward High Performance Ultracapacitors, *ACS Nano*, **2014**, *8*, 8255-65.

[47] Wu, D.; Xie, Z.; Zhou, Z.; Shen, P.; Chen, Z. Designing High-Voltage Carbonyl-Containing Polycyclic Aromatic Hydrocarbon Cathode Materials for Li-Ion Batteries Guided by Clar's Theory, *J. Mater. Chem. A.* **2015**, *3*, 19137-19143.

[48] "Graphene Chemistry: Theoretical Perspectives", John Wiley & Sons, 2013, ISBN: 978-1-119-94212-2, edited by De-en Jiang and Zhongfang Chen.

[49] Jiang, D. E.; Chen, Z. Introduction, *Book chapter* in *Graphene Chemistry: Theoretical Perspectives*, edited by De-en Jiang and Zhongfang Chen, John Wiley & Sons, **2013**, Chapter 1

[50] Wu, D.; Gao, X.; Zhou, Z.; Chen, Z. Understanding Aromaticity of Graphene and Graphene Nanoribbons by Clar Sextet Rule, *Book chapter* in *Graphene Chemistry: Theoretical Perspectives*, edited by De-en Jiang and Zhongfang Chen, John Wiley & Sons, **2013**, Chapter 3

[51] Gao, X.; Zhao, Y.; Chen, Z. From Graphene to Graphene Oxide and back, *Book chapter* in *Graphene Chemistry: Theoretical Perspectives*, edited by De-en Jiang and Zhongfang Chen, John Wiley & Sons, **2013**, Chapter 13.

[52] Li, F.; Chen, Z. Graphene-Based Materials as Nanocatalysts, *Book chapter* in *Graphene Chemistry: Theoretical Perspectives*, edited by De-en Jiang and Zhongfang Chen, John Wiley & Sons, **2013**, Chapter 15

[53] Li, Y.; Chen, **Z.** Hydrogen Storage in Graphene, *Book chapter* in *Graphene Chemistry: Theoretical Perspectives*, edited by De-en Jiang and Zhongfang Chen, John Wiley & Sons, **2013**, Chapter 16

[54] Tang, Q.; Zhou, Z.; Chen, Z. Graphene-related Nanomaterials: Tuning Properties by Functionalization, *Nanoscale*, **2013**, 5, 4541-4583.

[55] Jing, Y. Zhou, Z. Cabrera, C. R.; Chen, Z. Graphene, Inorganic Graphene Analogs and Their Composites for Lithium Ion Batteries, *J. Mater. Chem. A.* **2014**, *2*, 12104-12122.

[56] Tang, Q.; Zhou, Z.; Chen, Z. Innovation and Discovery of Graphene-Like Materials via DFT Computations, *WIREs Computational Molecular Science*, **2015**, *5*, 360-379.

[57] Yang, L. M.; Ganz, E.; Chen, Z.; Wang, Z. X.; Schleyer, P. v. R. Four Decades of the Chemistry of Planar Hypercoordinate Compounds, *Angew. Chem. Int. Ed.* **2015**, 54, 9468-9501; *Angew. Chem*. **2015**, *127*, 9602-9637.

[58] Chen, Z.; Wu, J. I.; Corminboeuf, C.; Bohmann, J.; Lu, X.; Hirsch, A.; Schleyer, P. v. R.; Is C_{60} Buckminsterfullerene Aromatic? *Phys. Chem. Chem. Phys.* **2012**, *4*, 14886-14891.

[59] Feng, J.; Li, F.; Jin, P.; Liao, Y.; Chen, Z. Searching For New Members of C_{70} Homofullerenes by First-Principles Computations: Bent's Rule at Work on C_{70} Surface, *J. Theor. Comput. Chem.* **2013**, *12*, 1250097.

[60] Li, F.; Jiang, D. E.; Chen. Z. Computational Quest for Spherical $C_{12}B_{68}$ Fullerenes with "Magic" π-electrons and Quasi-planar Tetra-coordinated Carbon, *J. Mol. Mod.* **2014**, *20*, 2085.

[61] Huang, X.; Zhao, Z.; Su, Y.; Chen, Z.; King, R. B. Design of Three-shell Icosahedral Matryoshka Clusters $A@B_{12}@A_{20}$ (A=Sn, Pb; B=Mg, Zn, Cd, Mn), *Scientific Reports* **2014**, *4*, 6915.

[62] Hao, J.; Li, F.; Li, H.; Chen, X.; Zhang, Y.; Chen, Z.; Hao, C. Dynamic Motion of Lu Pair inside $C_{76}(T_d)$ Cage, *RSC Advance*, **2015**, *5*, 34383-34389.

[63] Jin, P.; Hou, J.; Tang, C.; Chen, Z. Computational investigation on the endohedral borofullerenes $M@B_{40}$ (M = Sc, Y, La), *Theor. Chem. Acc.* **2015**, *134*, 13.

[64] Jin, P.; Tang, C.; Chen, Z. Carbon Atoms Trapped in Cages: Metal Carbide Clusterfullerenes, *Coord. Chem. Rev.* **2014**, *270-271*, 89–111.

[65] Zhao, J.; Huang, X.; Jin, P.; Chen, Z. Magnetic Properties of Atomic Clusters and Endohedral Metallofullerenes, *Coord. Chem. Rev.* **2015**, *289-290*, 315-340.

[66] Liao, Y.; Cruz, C. L.; Schleyer, P. v. R.; Chen, Z. Many M©Bn Boron Wheels are Local, but not Global Minima, *Phys. Chem. Chem. Phys.* **2012**, *14*, 14898-14904.

[67] Liu, Y.; Zhao, J.; Li, F.; Chen, Z. Appropriate description of intermolecular interactions in the methane hydrates: an assessment of DFT methods, *J. Comput. Chem.* **2013**, *34*, 121.

[68] Ding, K.; Chen, B.; Fang, Z.; Zhang, Y.; Chen, Z. Why the Photocatalytic Activity of Mo-doped $BiVO_4$ Is Enhanced: a Comprehensive Density Functional Study, *PCCP*, **2014**, *16*, 3465-76.

[69] Ding, K.; Chen, B.; Li, Y.; Zhang, Y.; Chen, Y. Comparative Density Functional Theory Study on the Electronic and Optical Properties of $BiMO_4$ (M= V, Nb, Ta), *J. Mater. Chem. A*, **2014**, *2*, 8294-8303.

[70] Yang, S.; Chen, C.; Liu, F.; Xie, Y.; Li, F.; Jiao, M.; Suzuki, M.; Wei, T.; Wang, S.; Chen, Z.; Lu, X.; Akasaka, T. An *Improbable* Monometallic Cluster Entrapped in a Popular Fullerene Cage: $YCN@C_s(6)\text{-}C_{82}$, *Scientific Reports* **2013**, *3*, 1487.

[71] Song, L. C.; Wang, L. X.; Li, C. G.; Li, F.; Chen, Z. Synthetic and structural study on some new porphyrin or metalloporphyrin macrocycle-containing model complexes for the active site of [FeFe]-hydrogenases, *J. Organomet. Chem.* **2014**, *749*, 120–128.